The carbonate-hosted Gortdrum Cu-Ag(±Sb-Hg) deposit, SW Ireland: C-O-Sr-Nd isotopes and whole-rock geochemical signatures

Pedro Cordeiro [a,*], Anderson Matias dos Santos [b], Geoffrey Steed [c], Andressa de Araújo Silva [b], Patrick Meere [d], Loretta Corcoran [e], Antonio Simonetti [e], Richard Unitt [d]

[a] *Pontifical Catholic University of Chile, Department of Mining Engineering, Santiago, Chile*
[b] *Federal University of Paraná, Department of Geology, Curitiba, Brazil*
[c] *Cardiff University, School of Earth and Ocean Sciences, Cardiff, UK*
[d] *University College Cork, School of Biological, Earth and Environmental Sciences, Cork, Ireland*
[e] *University of Notre Dame, Department of Civil & Environmental Engineering & Earth Sciences, Notre Dame, USA*

ARTICLE INFO

ABSTRACT

The Gortdrum Cu-Ag(±Sb-Hg) deposit, consisted of a fault-controlled orebody (3.8 Mt @ 1.19 % Cu and 25.1 g/t Ag) formed at the base of the Irish Midlands basin, in Lower Carboniferous rocks laterally time equivalent to Navan Group rocks hosting the giant Navan Zn-Pb deposit, and form the base of the Irish Midlands basin. The ore body is hosted on the hanging-wall of the Gortdrum Fault either along strata or within a wedge of brecciated carbonate rocks. Vertical zonation based on predominant host rock, ore textures, sulfide assemblages, and whole-rock geochemistry allowed the detailing of three ore types: a) the lower ore, representing Cu sulfides hosted within basal carbonated siliciclastic rocks; b) the upper ore, representing Cu, Cu-Sb, and Hg sulfides hosted within upper calcareous rocks and; c) the vein-associated ore, dominantly hosted in the more competent upper carbonate rocks. The origin of the deposit is unambiguously related to the development of the Gortdrum Fault and its associated permeability, which allowed basement/basin-derived fluids to react with carbonates and induce copper-silver mineralization. The mineralogy, ore shoot geometry, and geochemical association of Gortdrum are shared with classic Zn-Pb Irish-type deposits such as Navan, Lisheen, Silvermines, and Tynagh (sub-seafloor replacement). In these Irish-type deposits, copper-silver mineralization is associated with the late stage of Zn-Pb mineralization and shares a common geochemical footprint with Gortdrum of anomalous Ag, As, Sb and Hg. Additionally, the C-O and Sr-Nd isotope range of Gortdrum and Navan samples overlap, indicating that mineralization processes in both deposits were ineffective in modifying the original host-rock signature. These similarities suggest that Gortdrum could represent a variation of Irish-type mineralization where late-stage Cu-Ag-Sb-bearing fluids succeeded in forming a deposit. Hypothetical early-stage Zn-Pb fluids a) never existed; b) deposited disseminated sulfides in country-rocks, c) formed an undiscovered resource or, d) deposited ore concentrations that were eroded off.

1. Introduction

The Gortdrum deposit (3.8 Mt @ 1.19 % Cu and 25.1 g/t Ag), now mostly mined out, is an uncommon example of an Irish Midlands mineral occurrence with important concentrations of Hg, As, Sb, and U (Steed, 1986). The deposit was discovered following soil anomalies around a limestone quarry carrying low-grade copper and an IP (Induced Polarization) survey which suggested a conductive source (Thompson, 1965). Gortdrum is also a rare case in the province, where mineralization is spatially and geographically associated with sub-volcanic rocks (e.g., mafic dykes) at the deposit scale, in themselves locally mineralized. Most ore host rocks, however, are fractured limestones, calcareous marls, and calcareous shales from the Lower Limestone Shale Formation – a laterally and temporally equivalent to the Navan Group, host of the Navan deposit. The Gortdrum deposit is located within the hanging-wall of the ENE trending Gortdrum Fault, and has a strike length of 600 m, a perpendicular width of 100 m, and varies in thickness up to 120 m.

* Corresponding author.
E-mail address: pedro.cordeiro@ing.puc.cl (P. Cordeiro).

Rather than a metallogenic oddity of a small Cu-Ag resource within a world-class Zn-Pb province, Gortdrum highlights the potential for Cu deposits in the Irish Midlands. This world-class Zn-Pb province hosts deposits known as Irish type, such as the Navan, Lisheen, and Silvermines (110 Mt, 22 Mt, and 17 Mt of Zn and Pb resources, respectively, Andrew, 1986; Shearley et al., 1996; Ashton et al., 2015). The Irish type deposits form stratiform orebodies controlled by normal faults, contain mainly galena and sphalerite and minor chalcopyrite, arsenopyrite, and tennantite, and are hosted in Lower Carboniferous units (e.g., Fusciardi et al., 2004; Ashton et al., 2015; Kyne et al., 2019; Torremans et al., 2018). Lisheen and Silvermines are part of the Limerick Province, located in southwestern Ireland, and are host within dolomitic breccia in the Waulsortion micritic limestone Formation (e.g. Torremans et al., 2018). Some Zn-Pb occurrences spatially related to volcanic rocks are also observed in this part of Ireland, such as the mineralization at Stonepark (Elliott et al., 2015; Elliott et al., 2019). The Navan deposit is located in the North Midlands Province and hosted in the Navan Group, an argillaceous limestone on the top of Red Beds, and stratigraphically equivalent to the south Lower Limestone Shale Formation (e.g. Anderson et al., 1998; Ashton et al., 2015; Torremans et al., 2018). These Zn-Pb deposits were formed by mixing of metal-bearing hydrothermal fluids with sulfur-bearing shallow brines within roughly contemporaneous shallow ramp marine carbonates (Wilkinson, 2014). The deposition of various sulfide phases was predominantly stratabound, however, mixing of these fluids took place along dominantly vertical extensional structures. A range of Cu-bearing minerals such as chalcopyrite and tennantite in the Navan and Lisheen deposits occur in the ore zone proximal to the feeder fault, whereas they are largely absent in distal ores (Torremans et al., 2018; Yesares et al., 2019). This variation suggests a metal zoning pattern reflecting the migration of mineralization away from feeders within faults through permeable stratabound host horizons (Wilkinson, 2014). Also, there are some sea-floor replacements with Zn-Pb and Cu-Ag association (Maghfouri et al., 2020; Maghfouri and Hosseinzadeh, 2018; Maghfouri et al., 2019; Yesares et al., 2022). However, Gortdrum remains the only orebody mined in the Irish Midlands primarily for Cu, with Hg and Ag as by-products, but no significant Zn and Pb.

Additional Irish Cu-Ag occurrences similar to Gortdrum, such as Tullacondra (Silva et al., 2021), Ballyvergin (Andrew, 1986), and Aherlow (Romer, 1986) indicate regional metallogenic potential rather than an exotic occurrence. Tullacondra, for example, is an Irish carbonate-hosted Cu-Ag deposit containing a non-compliant legacy resource of 4.2 Mt @ 0.7 % Cu and 27.5 g/t Ag (Wilbur and Carter, 1986). Tullacondra is characterized by copper and silver mineralization hosted in the same stratigraphic unit of Gordtrum (Lower Limestone Shale), showing stratabound and vertical mineralized zones (Wilbur and Carter, 1986; Silva et al., 2021). Thus, a mineral system capable of concentrating copper and silver developed in the province, but its potential for deposits of large endowment is unknown. A detailed understanding of the Gortdrum ores and their geochemistry can be used to test a possible genetic relationship with the Irish-type mineralization system. This knowledge could be used in exploration to vector towards feeder zones, controlling structures and areas of increase potential for stratabound ores.

This work presents a detailed account of the textural and whole-rock geochemical association of the Gortdrum deposit, hydrothermal and ore minerals and their distribution within host rocks, metal zonation, and genetic implications. We also provide C-O and Sr-Nd isotope results from ore and barren samples to address the deposit genesis compared with other Irish examples, like Tullacondra Cu-Ag deposit (Wilbur and Carter, 1986; Silva et al., 2021). We discuss the main controls on copper and silver mineralization in Gortdrum, how they relate to other ore formation processes in the Irish Midlands and how this knowledge impacts mineral exploration efforts.

2. Geological setting

The Gortdrum deposit is located along the edges of the Irish Midlands Basin, right over the contact with the Munster Basin (Fig. 1) (Pickard et al., 1994). These basins formed over dominantly Paleozoic basement containing the Iapetus Suture; a suture zone associated with the closure of the Iapetus Ocean during the Caledonian Orogeny (Phillips and Sevastopulo, 1986). The onset of sedimentation was likely associated with post-Acadian extension in the Devonian period, and the basins were later inverted during the Late Carboniferous Variscan Orogeny (Ashton et al., 1986, 2015 and references therein).

The Munster Basin was deposited in the late Devonian during extension and subsidence of the dominantly Lower Paleozoic basement (Sevastopulo and Wyse Jackson, 2009). This subsidence was accompanied by northward marine transgression and the deposition of thick (up to 6 km) clastic Old Red Sandstone strata in the southwest of Ireland (Naylor and Shannon, 2011; Somerville et al., 2011). Sandstones, arkoses, and shales from the upper Munster Basin, associated with the Old Red Sandstone unit, marked the last siliciclastic-dominant input of the strata before the development of the Irish Midlands Basin conformably on top of the Munster Basin during a Lower Carboniferous marine transgression. Unlike the Munster Basin, the Irish Midlands Basin is predominantly carbonate-dominated with subordinate shales, in a sequence up to 1 km thick.

The base metal deposits of the Irish Midlands are dominantly hosted by the Waulsortian Limestone or the Navan Group, which overlie the Old Red Sandstone (Johnston, 1999). Both host units were deposited during the Carboniferous in the Tournaisian stage, from 359 to 347 Ma, and the consensus in the literature is that the large Zn-Pb deposits, such as Navan and Lisheen, were mainly formed between the Tournaisian and Visian ages, from 359 to 339 Ma (Wilkinson, 2003; Woodcock and Strachan, 2012; Hnatyshin et al., 2015). Therefore, mineralization is interpreted to have taken place after the development of limestones, although evidence for localized near-seafloor early-stage ore deposition is strong, particularly at Silvermines (Wilkinson, 2014). Ore formation ages are also nearly contemporaneous with regional rifting (NE-SW trending) across Europe and associated volcanism in Ireland and the British Isles (Woodcock and Strachan, 2012).

Magmatism in the Irish Midlands is recorded by the Lower Viséan to Chadian-Arundian (345–339 Ma) Knockroe Formation and by the Asbian (336–326 Ma) Knockseefin Formation as lava flows, pyroclastic deposits, and diatremes in western Ireland (Somerville et al., 1992; Elliott et al., 2015). Dikes and plugs generally associated with the Knockseefin Formation are hydrothermally altered and in close spatial relationship with Cu-Ag mineralization in Gortdrum (Steed, 1986) and Tullacondra (Wilbur and Carter, 1986).

3. The geology of the Gortdrum Cu-Ag($\pm$Sb-Hg) deposit

The Gortdrum deposit had an initial Cu-Ag reserve of 3.8 Mt @ 1.19 % Cu and 25.1 g/t Ag that was mostly mined out between 1965 and 1974. Although not realized at the start of operations, it also contained significant concentrations of Hg, which was also commercially extracted during the life of mine, together with As and Sb (Steed, 1986). Near the exhaustion of the mine resources, some U was also detected in the deepest part of the deposit (Duane, 1988). This geochemical footprint of Hg, As, Sb, and U was unique to Gortdrum, compared to other Irish Midlands deposits. Gortdrum is also exceptional in its spatial association with an important volume of sub-volcanic rocks at local and deposit scale. The ore geometry was primarily controlled by the ENE transcurrent Gortdrum Fault, with ore grade mineralization extending along a strike length of 600 m, a perpendicular width of 100 m, and varies in thickness of 120 m (Fig. 1b). Ores are hosted in basal dark limestones, calcareous marls, and calcareous shales of the Lower Limestone Shale Formation, temporally and laterally equivalent to the base of the Navan Group, which hosts the Navan deposit.
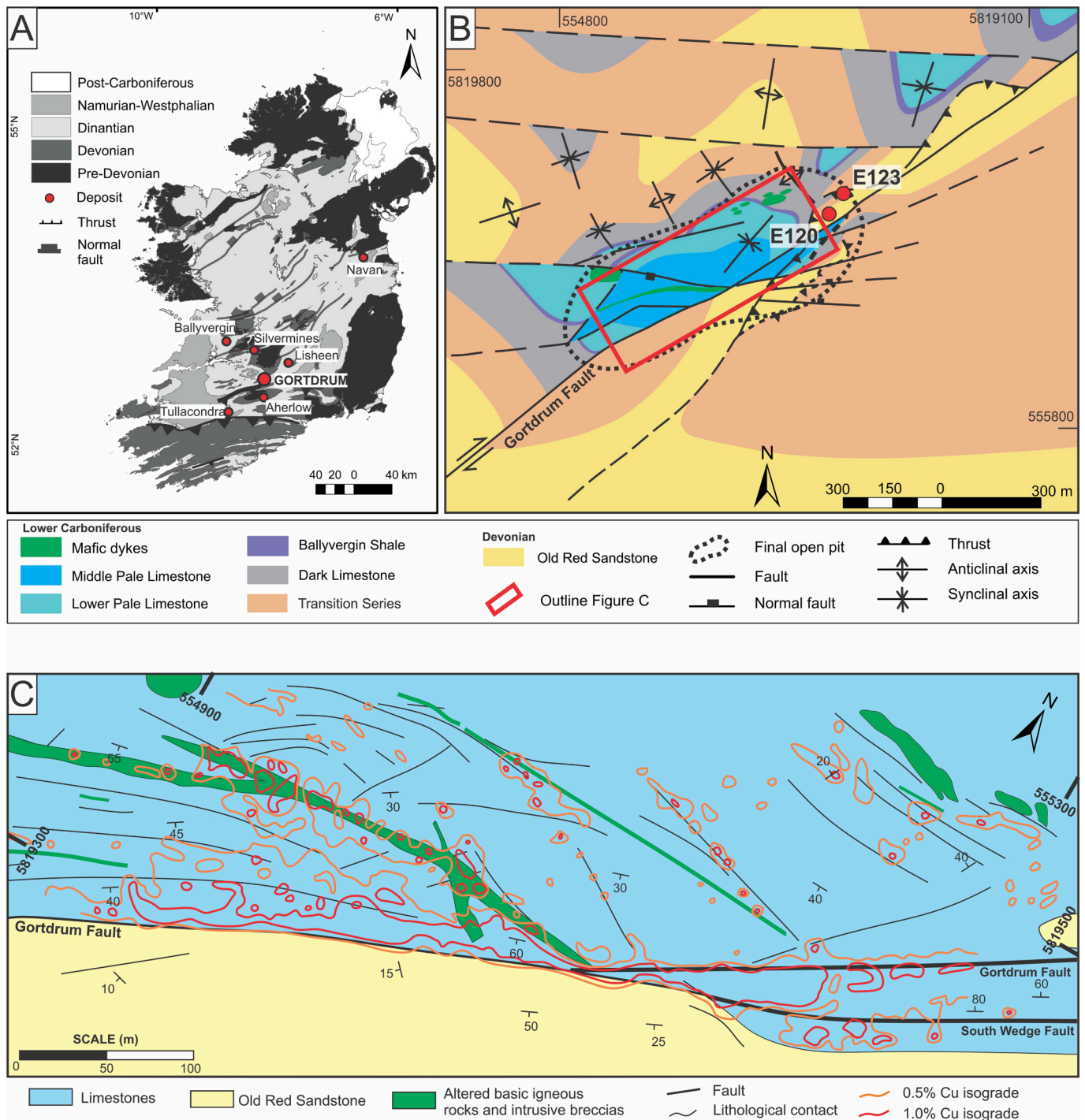
Fig. 1. a) Geological map of Ireland showing the main stratigraphic units and deposits relevant for the discussion; b) Geological map of the Gortdrum area showing the main units and structures overlain by the open pit outline, the location of drill holes sampled for this work and the outline of Fig. 1C (adapted from Gortdrum Mines Ltd., 1971); c) Geological map of the former Gortdrum Mine at Bench 3 displaying the main faults, dikes, plugs, dip direction and the 1 % and 0.5 % copper isogrades (from Steed, 1975).

3.1. Gortdrum stratigraphy

The stratigraphy of the Gortdrum deposit reflects the regional transition of the siliciclastic-dominant Old Red Sandstone into the carbonate-dominated Irish Midlands Basin (Fig. 2).

The **Old Red Sandstone units** are dominant at the footwall of the Gortdrum Fault and are divided from base to top into: a) Pale Sandstone: White medium-grained micaceous sandstone locally with crossbedding and conglomeratic beds of quartz and shale fragments; b) Red Shale and

Red Beds: ~3.5 m thick red-brown sandy shale; c) Gray sandstone: Interbedded gray and pink calcareous sandstones and shales. All sandstone varieties contain trace of calcite, mica, rutile, zircon, titanite, and tourmaline. Quartz is angular to subangular, with low sphericity and granulometry, and particle sizes vary from medium-grained to coarse at the base and fines upwards in the Pale Sandstone. Mica is fine-grained and a pervasive component of the matrix, estimated at ~10 % modal volume along with variable amounts of micritic calcite cement. This unit is rarely mineralized and sulfides (mainly chalcopyrite) sit within
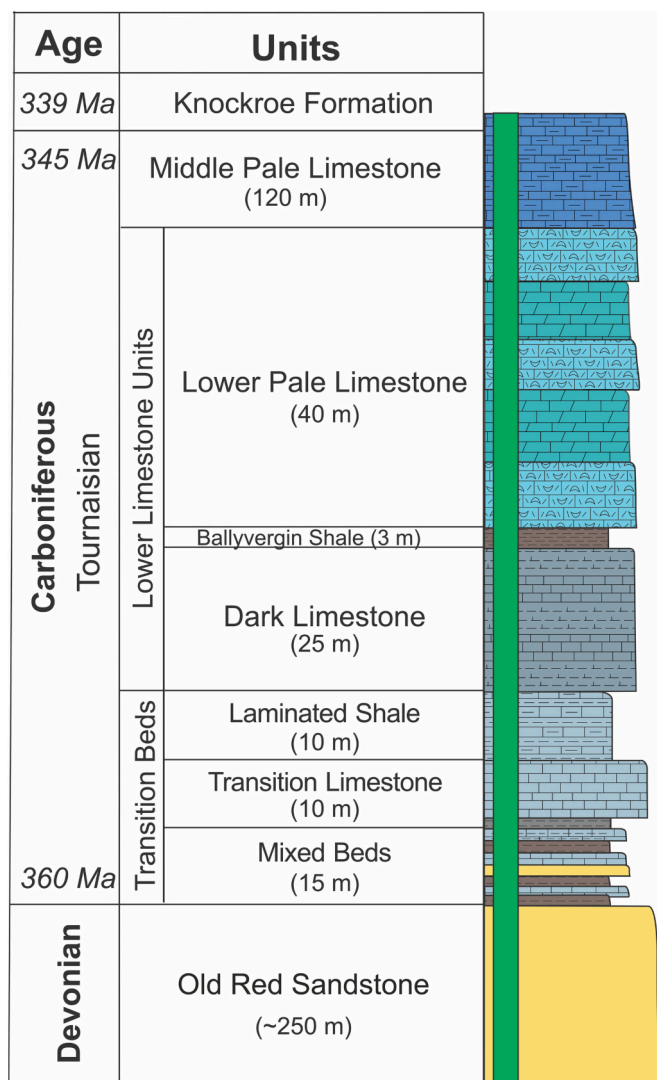
Fig. 2. Stratigraphic column of the base of the Irish Midlands Basin in the Gortdrum area. The main mineralization occurs in the Lower Pale Limestone (updated from Steed and Tyler, 1979).

micritic cement associated with dissolution seams.

The **Transition Beds** (or Mellon House Formation from Somerville and Strogen, 1992) are the basal unit of the Irish Midlands Basin and with around 30 m of thickness. It is divided into the: a) Mixed Beds: ~15 m thick interbedded strata that become carbonate-richer upwards and include calcareous sandstone, gray shale, black shale, marls and impure limestones; b) Transition Limestone: ~ 9 m thick uniform gray sandy limestone with <50 % very-fine quartz and minor amounts of rutile, mica and chlorite; c) Laminated Shale: <8 m thick interbedded calcareous marls to argillaceous marls with alternating dark gray and light gray beds, dependent on the content of fine-grained organic matter. The transition beds units can be differentiated from the underlying Old Red Sandstone units by a progressive increase in the modal content of carbonates, including beds with abundant bioclasts of echinoderms, and crinoids, albeit they are still dominantly siliciclastic.

The **Lower Limestone units** were deposited with a decreased siliciclastic input than the transitions beds, marking the transgression within the Irish Midlands Basin and its host most mineralization in Gortdrum. These units can be highly fractured, particularly near faults. At deposit level, this unit was divided into the: a) Dark Limestone - <25 m thick strata of dark gray bioclastic micritic limestone to calcareous marl interbedded with thin dark-gray shale to calcareous mudstones

with variable content of bioclasts and intraclasts; b) Ballyvergin Shale - <3 m thick uniform dark-gray shale interbedded with calcareous shales which represents an important marker horizon throughout the Lower Limestone Shale Formation/Navan Group (Strogen, 1988). Our samples from the Ballyvergin Shale show strong texture-destructive dolomitization and sulfide-replacement of bioclasts; c) Lower Pale Limestone (Lower Ballysteen Limestone of Silvermines) - <40 m thick light-gray, biosparitic to sparitic, oolitic and bioclastic, medium to coarse calcarenites to argillaceous calcarenites interbedded with black shales. These highly fractured calcarenites contain sub-rounded calcite ooids within sparitic calcite cement, and trace of quartz, cut by carbonate veinlets. Dissolution seams, stylolites, and chalcedony replacement are very common.

The **Knockroe Formation** is represented in the region by several trachyte stocks within 10 km west of the deposit and a roughly EW-trending swarm of 0.5–0.1 m thick mafic dikes (Steed, 1986). Around 120 m north of the Gortdrum Fault two 20–30 m wide pipe-shaped plugs composed of hydrothermally altered mafic rocks cut through the Lower Limestone Shale Formation and are interpreted in this work as part of the Knockroe Formation. These intrusions are spatially associated with igneous breccias of widely variable thicknesses from cm-scale up to 20 m thick (Steed, 1975), containing abundant clasts of host rocks and hydrothermally altered igneous rocks. The Gortdrum Deposit itself is cut by a swarm of 1 to 2 m thick ~EW trending dikes that merge into a 5 to 9 m thick composite zone of interlayered dikes and altered sedimentary rocks which are collectively referred to as the "Main Dike". Igneous breccias are conspicuous throughout the Gortdrum deposit and contain angular clasts of varied sizes set within a micritic matrix of quartz and muscovite. Dolomite-ankerite veining is ubiquitous within breccias and is associated with chalcedony and goethite. The majority of these veins cross-cut the breccia, however, there is a small subset of clasts of vein material suggesting a portion of the veins occurred prior to the onset of brecciation. Disseminated sulfides are present in both clasts and matrix. A couple of samples from Gortdrum igneous breccias reported by Steed (1986) are remarkably similar to maar diatreme-facies breccias from the Stonepark area, 20 km NW of Gortdrum (Elliott et al., 2015).

3.2. Structural geology and orebody geometry

The Gortdrum Fault zone within the deposit has a 0.5 to 5 m thick fault core and is oriented 335/75, up to sub-vertical locally, and has ~115 m of normal displacement (Steed, 1986). It is associated with a 15 m to 100 m thick damage zone forming a fractured limestone wedge sitting further north of the fault, at the eastern part of the mine grid, which hosts most of the mineralization (Figs. 1 and 3). The Gortdrum Fault extends 300 m southwest beyond the ore zone, and 5 km northeast as either barren rocks or containing low-grade Cu-Ag mineralization. Minor faulting is widespread within the Gortdrum orebody and includes ubiquitous normal and reverse faults with offsets from cm-scale to over 30 m. Open cylindrical folds occur in sandstones and limestones whereas clay-rich lithologies have irregular faulting or highly irregular ductile folding (Steed, 1986).

Ore geometry and fault style variations along the Gortdrum deposit allowed Steed (1975) to divide the orebody into two sections, separated by a pinch out zone where the Gortdrum Fault and the Main Dike-Wedge Fault intersect (Fig. 3). **The western orebody** hosts a swarm of mafic dikes collectively referred to as the Main Dike (Steed, 1975). **The eastern orebody** is composed of a wedge of shattered carbonate rocks, with subordinate altered igneous breccias, which is limited to the south by the South Wedge Fault, and to the north by the Gortdrum Fault. A secondary wedge is located between the South Wedge Fault and the South Branch Fault and it hosts peripheral mineralization. These wedges merge towards the eastern end of the orebody, coinciding with the end of the open pit. Low-grade ores follow the main trace of the Gortdrum Fault eastwards, that it has changed displacement along strike, where the Lower Limestone Shale Formation is thrusted over the Old Red
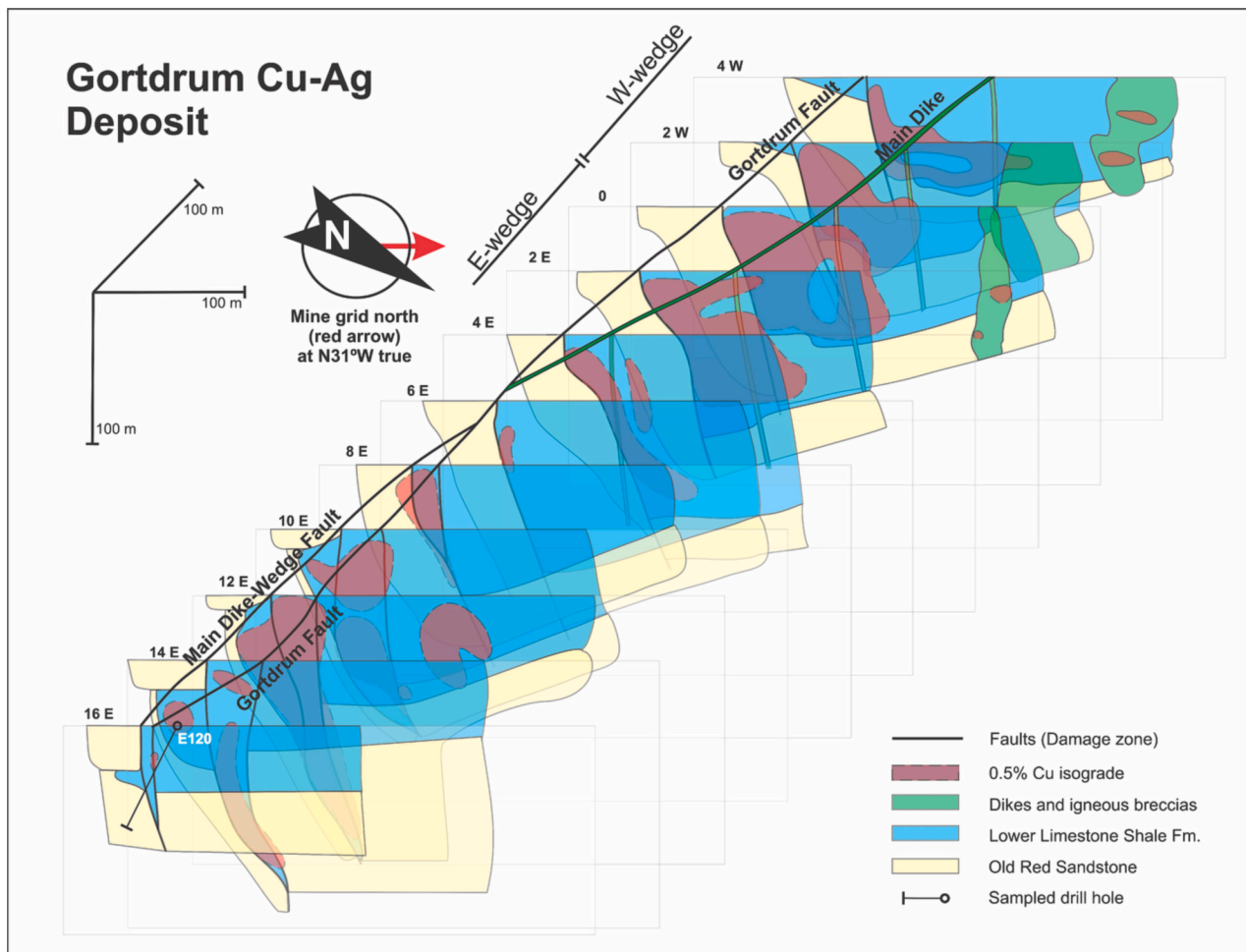
Fig. 3. Ore contour sections (0.5 % Cu) stacked along the Gortdrum Fault with main geological features highlighted and the location of drill hole E120, sampled for this work. Note that the western orebody formed between the Main Dike zone and the Gortdrum Fault whereas the eastern orebody sits within strongly faulted and fractured carbonate rocks between the wedge and the Gortdrum faults. Updated from Steed (1975) and legacy data from Gortdrum Mines.

Sandstone.

4. Methods

The mine geology described in this paper is based on data from Gortdrum Mines Ltd. between 1965 and 1972 which was provided to the Geological Survey Ireland (GSI) upon closure. Drill holes spacing was 25 to 50 m within the old open pit area and varied in exploration areas along strike from the Gortdrum Fault. Maps and sections presented here are modified versions from unpublished material based on mine geology mapping and historical Cu and Ag assay data (Steed, 1975). Systematic core sampling from holes E120 and E123 (Fig. 4), both drilled in the easternmost part of the open pit and stored at the GSI core shed, allowed the geochemical and petrographic assessment of ore bodies and host rocks. Mineral abbreviations used in figures follow the recommendations of Whitney and Evans (2010).

Twenty-eight selected samples were pulverized in a Widia pan mill at the Laboratório de Análises de Minerais e Rochas (LAMIR) of the Universidade Federal do Paraná (UFPR); between samples, the mill was decontaminated by milling with quartz. Whole-rock assaying was performed by ALS Global (ALS Global, 2016). Four acid digestion and ICP-AES finish allowed the determination of major oxides (SiO_2, Al_2O_3, Fe_2O_3, CaO, MgO, Na_2O, K_2O, Cr_2O_3, TiO_2, MnO, P_2O_5, SrO, BaO) and Ag, Cd, Co, Cu, Li, Mo, Ni, Pb, Sc, and Zn whereas LOI was determined through weight variation before and after furnace heating. Acid digestions (nitric, hydrochloric, and hydrofluoric acids) of fused beads and

analysis through ICP-MS were used to determine the contents of Ba, Ce, Cr, Cs, Dy, Er, Eu, Ga, Gd, Hf, Ho, La, Lu, Nb, Nd, Pr, Rb, Sm, Sn, Sr, Ta, Tb, Th, Tm, U, V, W, Y, Yb, and Zr. Arsenic, Bi, Hg, In, Re, Sb, Sc, Te, and Tl were analyzed by ICP-MS following aqua regia digestion. Total carbon and sulfur were analyzed using induction furnace. Detection ranges of relevant elements in our dataset are: Ag (0.01–100 ppm), As (0.1–250 ppm), Cu (0.2–10.000 ppm), Hg (0.005–25 ppm), Sb (0.05–250 ppm), U (0.05–250 ppm). Total carbon (C), total sulfur (S), and total organic carbon (TOC) were measured using a LECO analyzer and furnace.

Thirteen drill-core offcuts were selected as representative of the various lithologies and mineralization styles to produce qualitative elemental maps using an Edax Orbis micro-XRF instrument at the Center for Environmental Science and Technology (CEST), University of Notre Dame. Analytical parameters included a beam size of 30 μm, 40 kV and 300 μA current. The micro-XRF instrument generated elemental maps where various shades of gray indicated peak intensity for the analyzed elements which are relevant in this mineralizing system: Cu, S, Al, Fe, Ca, P, As, K, Mg, Mn, Si, Ti and Zn. Micro X-ray channels for Cu, Si, Ca, Fe and Al were merged into false colour RGB images generated using the ImageJ software. Extra care was taken to correspond elements versus colour channels to avoid overlap of colours between mineral phases. Determination of fine-grained sulfide and mineral phases was aided by semi-quantitative analysis through a SEM-EDS system JEOL EX-94410T1L11 from the LAMIR-UFPR with a spot size of 55 μm, under 20 kV, 100 nA and 30 s counting time. (For interpretation of the references to colour in this figure legend, the reader is referred to the web
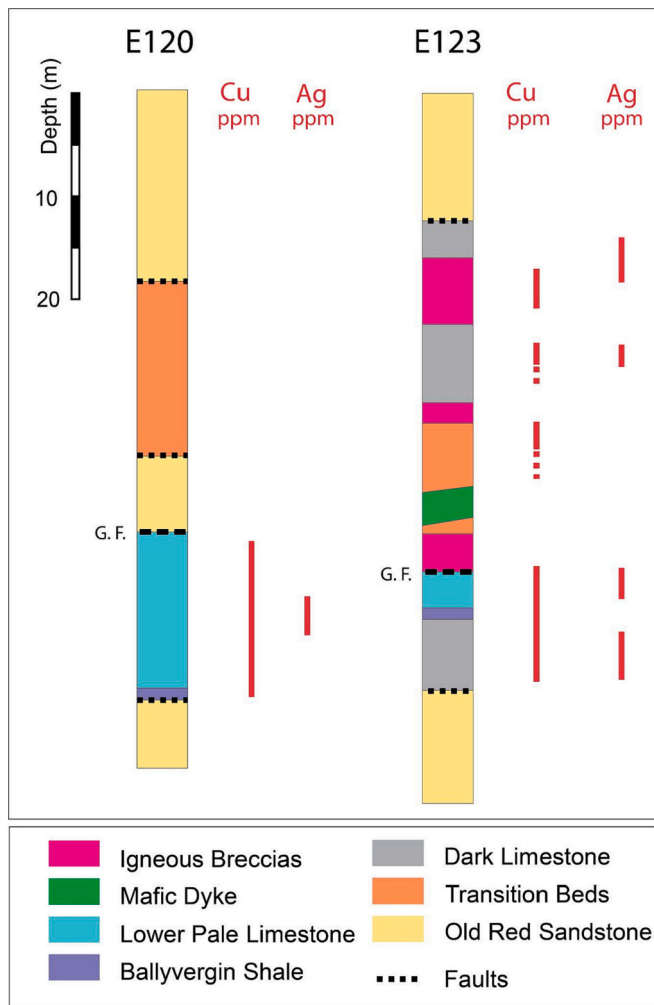
Fig. 4. Lithological units from the two drill-cores (E120 and E123), high-lighting the content of copper and silver (red line) at the ore host samples, and the mains faults/damage zone (G.F.: Gortdrum Fault). Note that the Lower Pale Limestone, Dark Limestone, and Igneous Breccias samples has significant Cu-Ag content. (For interpretation of the references to colour in this figure legend, the reader is referred to the web version of this article.)

version of this article.)

For C and O isotope investigation, whole-rock powder from Gortdrum (this work) and Tullacondra (Silva et al., 2021) from 40 samples were selected for analyses (Table 2). These samples were collected from three drill holes in the Tullacondra Cu-Ag deposit located in the western, central and western areas of the mineralized zone named as M73-3, M73-11 and M73-19 (Silva et al., 2021). Around 0.3 mg of powder was weighed, placed in sealed tubes, and followed by the addition of ~0.5 mL of concentrated H_3PO_4 (100 %). Samples were then thermally equilibrated at 100 °C using a Delta V Advantage isotope ratio mass spectrometer housed within CEST at the Notre Dame University, USA. Results are reported in per mil (‰), in delta notation as $\delta^{18}O$ and $\delta^{13}C$ values, and relative to the PDB (carbon) and SMOW (oxygen) standards. Three internal standards, YWCC, NBS 19, and ROYCC were used to validate and ensure the accuracy of the $\delta^{13}C$ and $\delta^{18}O$ results reported here (Table 2).

Additionally, the Sr and Nd isotope system were investigated for whole-rock powders from 14 samples from Gortdrum and Tullacondra (Table 3). For Sr isotope measurements, ion exchange columns held 1.7 mL of 200–400 mesh AG50W-X8 resin conditioned with 5 mL of 2.5 N DD HCl. The sample aliquot was then loaded onto the resin in 0.25 mL of 2.5 N HCl, washed with 9.75 mL 2.5 N HCl, and eluted with 4 mL of 2.5

N HCl. The Sr-bearing aliquots were dried down after ion-exchange separation. In sequence, these aliquots were taken-up in 2 % HNO_3 solution (~2 mL), aspirated into the ICP torch using the desolvating nebulizing system in a DSN-100 from Nu Instruments Inc. and strontium isotopes were measuring using a NuPlasma II MC-ICP-MS instrument according to the protocol in Balboni et al. (2016). For Nd isotope measurements, REEs were initially separated on 13.4 cm ion exchange columns containing 4.3 mL of 200–400 mesh AG50W-X8 resin. Subsequently, Nd was isolated in 9.7 cm columns with 1.22 mL of 50–100 mesh Eichrom Ln-Spec resin and measured using a Nu Plasma II MC-ICP-MS instrument. The same desolvating nebulizing system used for Sr isotope analyses was used for self-aspiration of the samples and JNd_i Nd isotope standard into the plasma. Measurements of ^{150}Nd, ^{148}Nd, ^{146}Nd, ^{145}Nd, ^{144}Nd, ^{143}Nd, and ^{142}Nd ion signals employed seven Faraday collectors in static/multi-collection mode. Analytical bias and drift and uncertainty measurements followed the procedure by Çimen et al. (2019).

5. Results

5.1. Ore types, textures, and mineralogy

Ores from the Gortdrum Deposit show relevant host rock features that could have influenced the conditions of sulfides precipitation. The mineralogy of the Lower Limestone unit, host of the Gortdrum mineralization, includes calcite, ferran-dolomite, dolomite, and sericite in carbonate rocks. In contrast, siliciclastic rocks (e.g., Old Red Sandstone Fm.), are primarily composed of quartz, muscovite, sericite, calcite, and ferran-dolomite with subordinate titanite, rutile, apatite, and monazite. The presence of localized to pervasive fabric-destructive dolomite to ferran-dolomite is a notable host rock feature in the Gortdrum Deposit. Several generations of dolomite and ferran-dolomite occur as elongated pods, in the matrix of breccias, comprising the bulk of the rock and as late-stage veins, which may carry ore minerals or be barren. Commonly, however, cross-cutting relationships are unclear and hinder a detailed paragenetic sequence of various dolomite phases.

The widespread occurrence of dissolution seams cutting through carbonate rocks (Fig. 5a and b), and siliciclastic rocks with carbonate cement is another conspicuous ore feature. Dissolution seams are roughly planar to rugged surfaces which vary from individual surfaces a few millimeters thick to multiple surfaces. These seams can be bedding-parallel or, more often, bedding oblique, and the dissolution is made clear by open space in clasts and matrix of the host rock infilled with euhedral dolomite and/or sulfides. The dissolution seams insoluble residue contains euhedral dolomite, chalcedony/quartz, organic matter, sericite, and subordinately, sulfides (Figs. 5 and 7). A striking feature of these seams is the variable abundance of sericite.

Apart from dolomite and sericite, calcite is another abundant mineral in Gortdrum forming the majority of the micritic matrix in carbonate-dominated rocks and, alternatively, as late-stage calcite and calcite-dolomite veins. Quartz is also ubiquitous as equigranular disseminated crystals and as euhedral overgrowths, except in the Lower Pale Limestone unit where it is largely limited to fine grains within shale beds. Muscovite is also abundant in siliciclastic rocks and, unlike sericite, it is coarser grained and bedding-parallel.

The main types of mineralization are: (a) disseminated (Fig. 5a and b), (b) concentrated along dissolution seams or bordering them (Fig. 6b), (c) hosted in veins (Fig. 9a), (d) along vein margins (Fig. 9b). The ore minerals in the Gortdrum Deposit are tennantite, chalcopyrite, bornite, and chalcocite, but important minor phases include pyrite, cinnabar, cobaltite, native silver, amalgam (Hg-Ag), and stromeyerite, whereas galena and sphalerite are very rare. Associated gangue minerals are restricted to chalcedony and a euhedral calcite and Fe-dolomite.

Spatial variations of sulfide mineralogy reveal an important zonation whereby chalcopyrite is the dominant copper-iron sulfide in the center of the Gortdrum Deposit and bornite at the edges it is chalcopyrite

Table 2
C and O isotope data for whole-rock samples of Gortdrum and Tullacondra.

Sample	Deposit	Unit	$\delta^{13}C/^{12}C$ ‰ (PDB)	Uncertainty	$\delta^{18}O/^{16}O$ ‰ (SMOW)	Uncertainty
E120-090	Gortdrum	Mixed Beds	−2.67	0.06	18.10	0.06
E120-194	Gortdrum	Mixed Beds	−3.08	0.05	17.31	0.06
E123-085	Gortdrum	Lower Limestone Unit	0.29	0.05	18.95	0.08
E123-087	Gortdrum	Breccia	−1.42	0.04	18.20	0.06
E123-096	Gortdrum	Breccia	−1.87	0.06	18.03	0.06
E123-109	Gortdrum	Upper Transition Beds	0.71	0.05	18.40	0.07
E123-119	Gortdrum	Upper Transition Beds	1.12	0.05	19.28	0.06
E123-127	Gortdrum	Lower Limestone Unit	2.00	0.05	20.57	0.06
E123-134	Gortdrum	Breccia	−1.63	0.06	19.17	0.13
E123-144	Gortdrum	Upper Transition Beds	−0.33	0.06	19.00	0.09
E123-151	Gortdrum	Mixed Beds	−1.90	0.05	18.63	0.08
E123-160	Gortdrum	Lower Limestone Unit	−1.53	0.07	17.91	0.06
E123-170	Gortdrum	Mixed Beds	−2.65	0.04	18.35	0.06
E123-179	Gortdrum	Breccia	−2.02	0.07	17.66	0.08
E123-184	Gortdrum	Lower Limestone Unit	−1.41	0.03	18.19	0.05
E123-193	Gortdrum	Lower Limestone Unit	0.78	0.07	18.79	0.14
E123-201	Gortdrum	Lower Limestone Unit	1.02	0.04	19.08	0.04
E123-206	Gortdrum	Lower Limestone Unit	−0.16	0.03	18.80	0.03
E123-211	Gortdrum	Lower Limestone Unit	1.96	0.04	18.77	0.04
E123-215	Gortdrum	Lower Limestone Unit	0.37	0.03	19.08	0.05
M73-3-027	Tullacondra	Upper Limestone	1.85	0.03	23.84	0.03
M73-3-039	Tullacondra	Upper Limestone	1.59	0.02	21.56	0.04
M73-3-094	Tullacondra	Upper Limestone	1.70	0.04	19.98	0.06
M73-3-154	Tullacondra	Lower Limestone Unit	3.51	0.05	17.94	0.08
M73-3-162	Tullacondra	Lower Limestone Unit	2.95	0.06	20.34	0.09
M73-3-196	Tullacondra	Lower Limestone Unit	2.89	0.06	23.21	0.08
M73-3-203	Tullacondra	Lower Limestone Unit	2.02	0.04	19.94	0.04
M73-3-283	Tullacondra	Upper Transition Beds	0.01	0.03	17.59	0.04
M73-3-328	Tullacondra	Upper Transition Beds	−1.25	0.05	20.96	0.09
M73-3-393	Tullacondra	Mixed Beds	−0.17	0.08	20.06	0.06
M73-11-290	Tullacondra	Upper Limestone	3.92	0.06	21.13	0.14
M73-11-312	Tullacondra	Lower Limestone Unit	3.98	0.03	20.69	0.04
M73-11-319	Tullacondra	Lower Limestone Unit	4.37	0.03	20.95	0.04
M73-11-336	Tullacondra	Upper Transition Beds	4.59	0.03	21.44	0.05
M73-11-347	Tullacondra	Upper Transition Beds	3.85	0.03	21.61	0.05
M73-11-359	Tullacondra	Upper Transition Beds	2.11	0.04	20.56	0.05
M73-11-422	Tullacondra	Mixed Beds	0.14	0.07	18.82	0.07
M73-11-510	Tullacondra	ORS	−4.91	0.02	16.92	0.03
M73-19-72	Tullacondra	Mixed Beds	2.74	0.04	20.07	0.03
M73-19-133	Tullacondra	ORS	0.76	0.04	21.37	0.06

(Steed, 1975). However, our samples come from drill holes at the NE part of the deposit where vertical zonation is dominant, as suggested by the predominance of limestone-hosted tennantite and chalcopyrite over other sulfide phases in the upper ore, contrasting with the near absence of tennantite in siliciclastic-hosted ores. Additionally, dolomite and calcite veins cutting through both barren rocks and ore zones may carry ore minerals that reflect the composition of host rocks. Based on ore texture, mineralogy, and host unit, we can distinguish three ore types: a) **Upper ore**; b) **Lower ore**; c) **Vein-associated ore**.

5.1.1. Upper ore

The upper ore is predominantly hosted within strongly fractured limestones, marls, and calcarenites of the Lower Limestone units (Fig. 5a and b) and contains fine- to medium-grained tennantite, bornite, and chalcopyrite (Fig. 6); typically, with tennantite being the most common sulfide. Additionally, the ratio of bornite/chalcopyrite is observed to be higher in the center of Gortdrum compared to the edges of the deposit where chalcopyrite dominates, based on the company data. Upper ore sulfides are characterized by disseminations replacing calcite within carbonate-rich domains but they may also be spatially associated with dissolution seams (Figs. 5, 6b, f).

Tennantite forms anhedral to subhedral disseminated crystals up to 5 mm wide replacing carbonates (Fig. 6a to g). The majority of bioclast are chalcedony. EDS analyses suggest the dominance of As over Sb in the tennantite structure and the variable occurrence of Hg and Ag, thus supporting the earlier electron microprobe analyses given by Steed (1975). Tennantite alongside chalcopyrite replaces bioclasts in the Dark Limestone in a similar manner to chalcedony replacement, as seen by the

rounded and curved texture of the ore minerals indicating bioclastic pseudomorphs (Fig. 6a). Chalcopyrite and bornite are also fine- to coarse grained, subhedral, and commonly enveloped by tennantite (Fig. 6c, d, e, g). Chalcocite occurs as very fine grains rimming bornite crystals (Fig. 6e and g) and as very fine-grained inclusions within bornite and tennantite. Cinnabar occurs in trace amounts and is very fine-grained, or as filling porosity space (Fig. 6h) or alternatively as conspicuous red staining, especially on fractures. According to EDS analyses, mercury amalgam within limestone fracture fills contain Ag. Other subordinate upper ore minerals may include pyrite, argento-tennantite (Fig. 6e), galena (Fig. 6e and g), covellite, stromeyerite (AgCuS, Fig. 6e), and gortdrumite-$Cu_{24}Fe_2Hg_9S_{23}$ (Fig. 6d), for which Gortdrum is the type location (Steed, 1983).

5.1.2. Lower ore

The lower ore is dominated by bornite and/or chalcopyrite replacing both matrix carbonates and bioclasts in calcareous shales, marls, and impure limestones of the Transition Limestone and the Laminated Shale. Sulfide abundance drops sharply in the basal Mixed Beds and is only rarely hosted within the Old Red Sandstone. Sulfides have been precipitated either disseminated around or within bedding, bedding-parallel/oblique dissolution seams (Fig. 7a and b).

Lower ore copper sulfides are dominantly spatially associated with dolomite and/or with sericite-rich domains which commonly sit along bedding or dissolution seams (Figs. 7a, 8a, and b). In mine outcrops, high grade lower ore could be traced down dip for several meters in association with pervasive dolomitization, or replacement of calcite, concentration of matrix sericite along dissolution seams, and the

Table 3
Sr and Nd isotope data for whole-rock samples of Gortdrum and Tullacondra.

Sample	Deposit	Unit	Depth (m)	Rb (ppm)	Sr (ppm)	$^{87}Rb/^{86}Sr$	2σ	$^{87}Sr/^{86}Sr$	$^{87}Sr/^{86}Sr$ (i)	Sm (ppm)	Nd (ppm)	$^{147}Sm/^{144}Nd$	$^{143}Nd/^{144}Nd$	2σ	$^{143}Nd/^{144}Nd$ (i)	ε Ndt
E123_85	Gortdrum	Lower Limestone Unit	25.9	72	195	1.072488347	0.00001	0.7160592	0.710791111	4.92	24.2	0.125936921	0.51219	0.00001	0.5119023	−5.563156726
E123_109	Gortdrum	Upper Transition Beds	33.2	99	278	1.031739576	0.00001	0.7152488	0.71018087	5.25	26.5	0.121502435	0.51212	0.00001	0.511838862	−6.801724023
E123_144	Gortdrum	Upper Transition Beds	43.9	60	154	1.128684329	0.00001	0.7160636	0.710519475	4.6	24.7	0.116720771	0.51207	0.00001	0.51180622	−7.439034585
E123_160	Gortdrum	Lower Limestone Unit	48.8	110	269	1.184731938	0.00001	0.7134812	0.707661768	13.55	69.3	0.12455596	0.51256	0.00001	0.512273065	1.675692894
E123_184	Gortdrum	Lower Limestone Unit	56.1	31	194	0.468929559	0.00001	0.7135989	0.711295506	2.64	10.3	0.159304227	0.51219	0.00001	0.511823235	−7.106835251
E123_201	Gortdrum	Lower Limestone Unit	61.3	25	247	0.292066728	0.00007	0.7110995	0.709664861	5.63	21.2	0.162253377	0.51224	0.00001	0.511868777	−6.217674817
E123_211	Gortdrum	Lower Limestone Unit	64.3	29	361	0.232739709	0.00001	0.7102599	0.709116677	3.53	15.8	0.138329311	0.51217	0.00001	0.511848002	−6.623289948
M73_3_162	Tullacondra	Lower Limestone Unit	49.4	78	71	3.184466697	0.00001	0.7271417	0.711499521	8.55	44	0.11966598	0.51240	0.00001	0.512123871	−1.237187482
M73_3_393	Tullacondra	Mixed Beds	119.8	130	17	21.64580767	0.00001	0.8211805	0.71485576	10.15	46.7	0.133381065	0.51195	0.00001	0.511640441	−10.67572383
M73_11_290	Tullacondra	Upper Limestone	88.4	79	437	0.525740509	0.00001	0.7118437	0.70926125	3.58	16.8	0.131479794	0.51192	0.00001	0.511621798	−11.0397193
M73_11_319	Tullacondra	Lower Limestone Unit	97.2	10	486	0.058421069	0.00001	0.7095396	0.709252634	1.65	7.7	0.135854761	0.51200	0.00001	0.511688572	−9.736004521
M73_11_422	Tullacondra	Mixed Beds	128.6	103	460	0.648722684	0.00001	0.711626	0.708439458	5.85	28.8	0.127182232	0.51202	0.00001	0.511724446	−9.035593551
M73_19_133	Tullacondra	ORS	40.5	15.2	442	0.099632496	0.00004	0.7118909	0.711401503	5.95	26	0.143966687	0.51206	0.00001	0.511731883	−8.890404875
M73_19_249	Tullacondra	ORS	75.9	125	21	17.50982567	0.00001	0.8158111	0.729802405	4.66	26.1	0.112285741	0.51187	0.00001	0.511611984	−11.23133115

preservation of quartz- and clay-rich bands (Steed, 1975).

Chalcopyrite in the lower ore is very fine- to fine-grained and commonly filling voids with euhedral calcite or dolomite (Fig. 8d). Pyrite is rare and limited to framboidal crystals wrapped by chalcopyrite (Fig. 8e). Tennantite and covellite are uncommon and show an undefined cross-cutting relationship with chalcopyrite (Fig. 8c).

5.1.3. Vein-associated ore

The vein-associated ore occurs in veins with thicknesses up to 20 cm veins (Type 1), or ca. 3 cm thick veins, containing fine-grained subhedral ferroan-dolomite and calcite (Fig. 8a), and are largely hosted within rocks of the Lower Pale Limestone unit or within igneous breccias (Fig. 9b). Type 1 veins contain coarser (up to 10 cm) tennantite and chalcopyrite compared with upper ores (Fig. 9c to e). Sulfides are generally within veins, but they may also be hosted within the host rock together with Type 1 veins. Some sulfide-bearing veins also cut through dikes (Steed, 1975). Types 2 and 3 veins are posterior, calcite-dominant, and barren.

6. Whole-rock geochemistry

Results of whole-rock geochemistry from ore and barren samples of the Gortdrum deposit indicate important chemical differences between ore types and between various host units (Fig. 10). The data were divided into groups of stratigraphic units, from bottom to top: a) Old Red Sandstone; b) Mixed Beds; c) Upper Transition Beds, encompassing the Laminated Shale and Transition Limestone units, and; d) Lower Limestone Units, encompassing the Ballyvergin Shale, and Lower Pale, and Dark limestone units. Additionally, samples with a positive correlation between Cu and S (Cu > 0.1 %) were labeled as mineralized, whereas those lacking this correlation but with Cu < 0.1 % Cu were labeled as barren.

The mineralogical variation within the Gortdrum Deposit strata correlates with the composition of the major elements in the minerals. This correlation can be mainly exemplified by the variation of siliciclastic and carbonatic material by SiO_2 and CaO wt% values, respectively, from the Old Red Sandstone (SiO_2 93.5–83.5 %; CaO 1.53–0.29 %) to the Mixed Beds (SiO_2 61.5–43 %; CaO 18.2–7.68 %) to the Dark and Lower Pale limestone units (SiO_2 45.2–8.36 %; CaO 46.2–22 %). The content of MgO, which largely reflects the dolomite content of the host rock, varies throughout stratigraphic units, however, it is always below 6 %. The MgO content shows a moderate positive relationship with MnO (up to 0.5 %) and Fe_2O_3 (up to 8 %) and lacks a clear correlation with the Cu content (Fig. 10). The Al_2O_3 contents, on the other hand, are directly related to the amount of clay, sericite, and feldspar in the host rock and show a strong positive correlation with K_2O for all rock types, samples with <0.3 % TiO_2 (above 0.3 %, correlation is lacking due to interference of detrital minerals) and various other trace elements such as Rb, Cs, Nb, Ta, Ga, and Th. Both K_2O and Al_2O_3 show positive correlations with minor elements such as Ba, V, Cr, Zr, and Hf, albeit with more scatter (Table 1). Finally, Duane (1988) reports uranium minerals associated with the propylitic alteration of dikes in Gortdrum. These dikes were not part of our sampling set, and we did not detect any important uranium concentrations.

In terms of chalcophile elements, Gortdrum Deposit ores are characterized by high Cu, Ag, S, Sb, As and Hg (Fig. 10). Of particular note is the high abundance of As, Sb, Hg and Ag in the upper ore (As > 250 ppm, Sb > 100 ppm, Hg > 250 ppm, Ag 4–16 ppm) and their near absence in the lower ore (As 31–11 ppm, Sb 1.3–3 ppm, Hg 4–14 ppm, Ag 1–1.6 ppm). The strong U enrichment observed within igneous breccias in the same area of our sampling (Duane, 1988) was lacking in our samples as U concentration was <7 ppm.

7. C-O and Sr-Nd isotopes

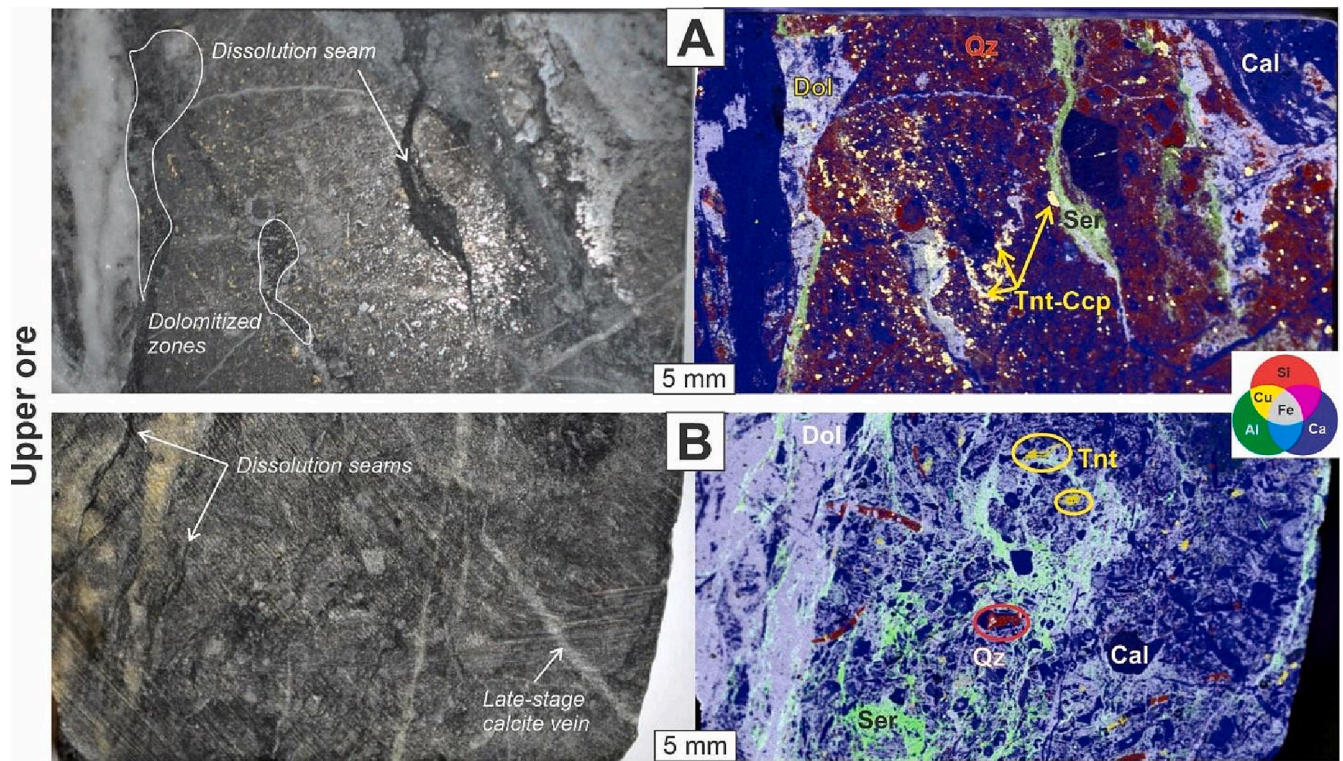The C-O and Sr-Nd isotope signatures from Gortdrum vary

Fig. 5. Upper ore textures displayed on core samples (on the left) and equivalent areas imaged by micro-XRF as false colour compositions (on the right). a) Calcareous sandstone from the Dark Limestone unit showing disseminated medium-grained tennantite (tnt) and chalcopyrite (ccp) within the quartz-rich (qz) matrix. Sericite-rich (ser) domains in dissolution seams, dolomitized zones and late-stage calcite (cal) veins are sulfide poorer in comparison to matrix disseminations (E123-085). b) Lower Pale Limestone with calcite intraclasts within the dolomite (dol) matrix, sericite-domains in dissolution seams, and disseminated tennantite (E123-201). (For interpretation of the references to colour in this figure legend, the reader is referred to the web version of this article.)
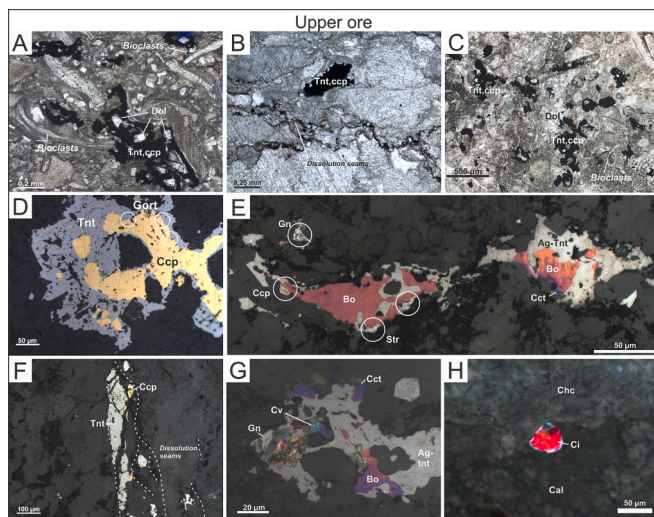

Fig. 6. Upper ore photomicrographs. a) Tennantite (tnt) and chalcopyrite (ccp) containing euhedral dolomite and replacing micritic calcite matrix and bioclasts (chalcedony) (E120-190); b) Sulfides spatially associated with dissolution seams (E120-173); c) Disseminated tennantite and chalcopyrite replacing bioclasts and the matrix (E123-211); Photographies a), b) and c) are in transmitted plane-polarized light (TPPL). d) Chalcopyrite rimmed by tennantite and very fined-grained gortdrumite (gor) (E123-211); e) Bornite (bo) crystals rimmed by tennantite, chalcopyrite, and stromeyerite (str) (E123-201); f) Copper sulfides along dissolution seams (E123-184); g) Ag-tennantite interlocked with covellite (cv), bornite, chalcocite (cct), and galena (gn) (E123-211); h) Cinnabar (ci) with chalcedony (chc) and calcite (cal) (E123-201). Photographies d), e) and f) are in reflected plane-polarized light (RPPL).

consistently between different units and have a compositional range compatible with that from the Navan Zn-Pb deposit (Ashton et al., 2015), also hosted at the lowest units of the Irish Midlands Basin. However, considering the metallic differences between Navan and Gortdrum, a comparison with a Cu-Ag deposit in the province would be beneficial. We also used the isotopic results from the Tullacondra Cu-Ag deposit for comparison (Wilbur and Carter, 1986; Silva et al., 2021). Whole-rock geochemistry results also indicate similar geochemical ranges between Gortdrum (this work) and Tullacondra (Silva et al., 2021).

The whole-rock C and O isotope results from Gortdrum ($\delta^{18}O_{SMOW}$ = 17.3 ‰ to 20.5 ‰; $\delta^{13}C_{PDB}$ = −3.0 ‰ to 1.9 ‰) are characterized by much lower $\delta^{13}C_{PDB}$ and $\delta^{18}O_{SMOW}$ values for the ORS and Mixed Beds units compared with the carbonate-rich ones above them (Lower Limestone Units). Results from Tullacondra ($\delta^{18}O_{SMOW}$ = 16.9 ‰ to 23.8 ‰; $\delta^{13}C_{PDB}$ = −4.9 ‰ to 4.6 ‰) agree with those from Gortdrum where carbonate-dominated upper units have higher C and O isotope values but show a much wider spread of oxygen isotope compositions. The data also suggests systematically higher C and O isotopic values for Tullacondra compared with Gortdrum. On the other hand, mineralized samples from both deposits lack significant C-O isotopic differences from barren ones. Carbonate-dominant samples from both Gortdrum and Tullacondra show similar C-O isotopic ranges with Navan stage 2 calcite vugs associated with the main mineralization stage of Navan and the sulfide deposition (including chalcopyrite) (Fig. 11a).

The whole-rock Sr and Nd isotope data from Gortdrum and Tullacondra are listed in Table 3, and depicted in Fig. 11b. The age of 350 Ma, interpreted as the estimated age of mineralization for Navan (Walshaw et al., 2006), has been adopted to calculate initial ratios. Gortdrum samples display a small range of initial $^{143}Nd/^{144}Nd$ ratios (from 0.51190 to 0.51181) and initial $^{87}Sr/^{86}Sr_{(350\ Ma)}$ ratios (0.7113 to 0.7091), except for a sample (E123-160) of mineralized Ballyvergin
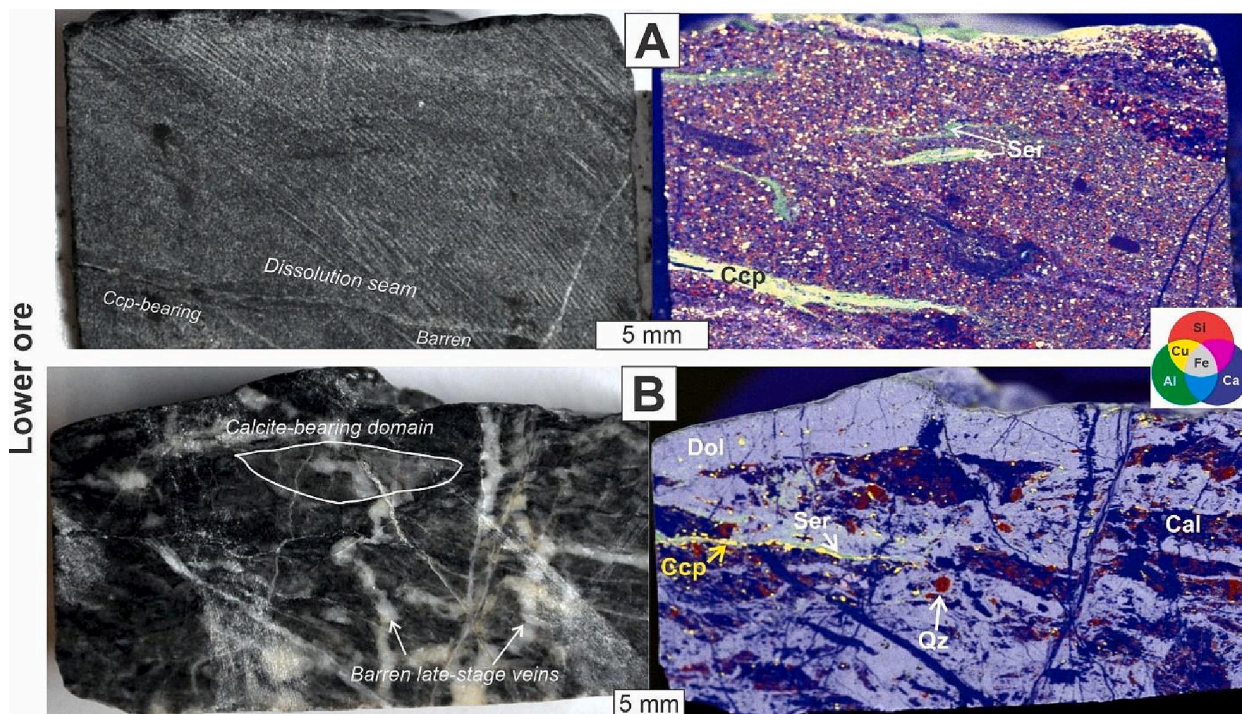
Fig. 7. Lower ore samples with textures highlighted on core samples (on the left) and equivalent areas imaged by micro-XRF as false colour compositions (on the right). a) E123-144 Medium-grained calcareous sandstone from the Laminated Shale Unit showing chalcopyrite (ccp) dominantly along dissolution seams and disseminated in the calcite matrix. Sericite-bearing (ser) seams may contain chalcopyrite or be barren. b) Dolomite (dol) limestone from the Transition Limestone Unit E123-184 showing sericite- and chalcopyrite-bearing dissolution seams and disseminated along the contact of calcite and dolomite domains. (For interpretation of the references to colour in this figure legend, the reader is referred to the web version of this article.)
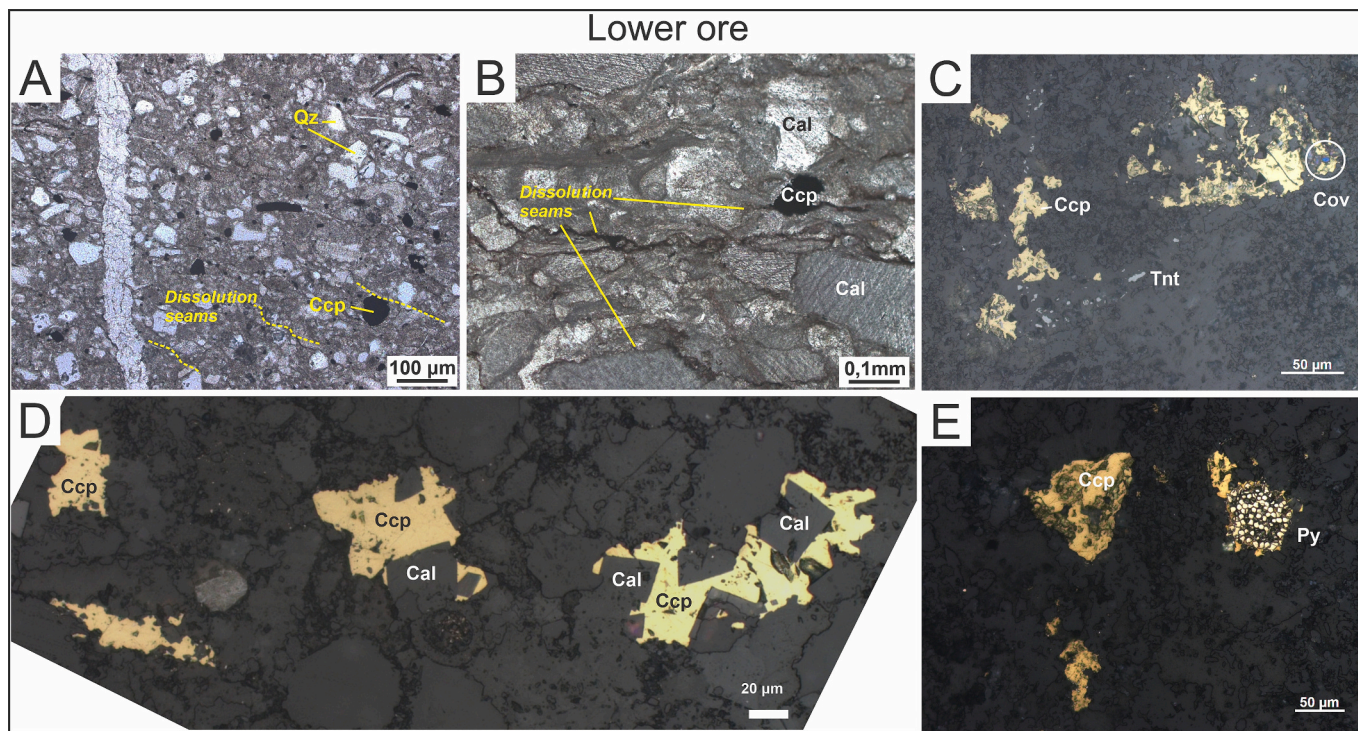

Fig. 8. Lower ore photomicrographs. a) Disseminated chalcopyrite (ccp) spatially associated with incipient dissolution seams within carbonate and quartz (qz) in the matrix. A small vein cutting the sample in the right (E123-144). b) Detail of the spatial relationship of dissolution seams, chalcopyrite and calcite (cal) (E123-085). Photomicrographs a) and b) are in TPPL. c) Rare association of chalcopyrite, tennantite (tnt) and covellite (cov) (E123-085). d) Chalcopyrite fillings voids with euhedral calcite (E123-144). e) Chalcopyrite overgrowing framboidal pyrite (py) (E123-085). Photomicrographs c), d) and e) are in RPPL.
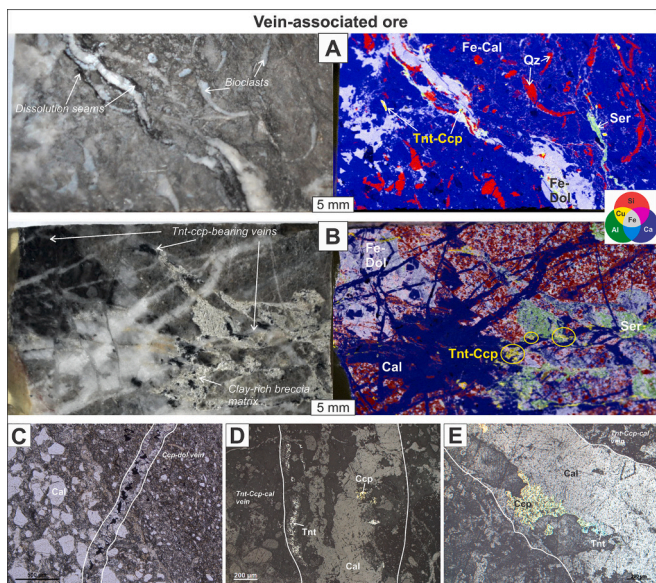
Fig. 9. Images a) and b) show vein-associated ore samples with textures highlighted on core samples (on the left) and equivalent areas imaged by micro-XRF as false colour compositions (on the right). a) Lower Pale Limestone calcarenite showing silicified bioclasts within ferroan-calcite matrix cut by ferroan-dolomite veins carrying tennantite and chalcopyrite. Sericite domains sit along dissolution seams cutting bioclasts (E120-165); b) Igneous breccia within the Dark Limestone Unit showing a calcareous sandstone cut by clay-rich domains and calcite veinlets with tennantite and chalcopyrite (E123-087). c–e) Photomicrographs from aspects of Gortdrum Type 1 veins: c) Chalcopyrite-dolomite vein cutting calcarenite (E123-096). Photomicrograph in TPPL; d) Chalcopyrite-tennantite calcite vein (E123-096); e) Association of chalcopyrite and tennantite within a calcite vein (E120-167). Photomicrographs d) and e) in RPPL. (For interpretation of the references to colour in this figure legend, the reader is referred to the web version of this article.)

Shale with anomalous compositions (0.512273 and 0.7077, respectively). Tullacondra samples have a similarly restricted range of initial $^{143}Nd/^{144}Nd$ ratios (from 0.51173 to 0.51161), but more variable initial $^{87}Sr/^{86}Sr$ ratios (0.7298 to 0.7084). Again, a single sample (M73-3-162) shows anomalous compositions (0.512123 and 0.7114, respectively), this time from the top of the Lower Limestone Unit underneath the Ballyvergin Shale. When anomalous compositions are disregarded, the data suggests that Gortdrum Sr-Nd compositions are similar to those from barren Old Red Sandstone and Silurian metasedimentary rocks reported by Walshaw et al. (2006). Tullacondra compositions, on the other hand, have lower $^{143}Nd/^{144}Nd$ ratios compatible with data from Navan gangue, but the spread in $^{87}Sr/^{86}Sr$ ratios observed for the Old Red Sandstone literature data are the same in Tullacondra. Similar to the C and O isotopic data, our Sr-Nd isotopic data cannot differentiate between mineralized and barren samples in either deposit. Samples with anomalous Nd isotope results also indicate a tendency for higher Nd values (40 to 70 ppm) compared with the majority of our dataset where Nd < 30 ppm (Fig. 11c). These samples with anomalous Nd isotope results also show higher Nb, Ta, Y, Zr, and Th contents than others (Table 1).

8. Discussion

The textural and mineralogical associations of the Gortdrum Deposit allow the proposal of a paragenetic sequence that includes five stages: sedimentary, diagenetic, *syn*-ore, late-ore, and post-ore (Fig. 12). The sequence highlights the multi-stage evolution of Gortdrum and the variety of sedimentary, post-depositional, and ore formation processes that took place to form the deposit.

8.1. Dolomitization

Dolomite in the Gortdrum Deposit, as investigated through petrography and micro-XRF, occurs in a variety of sedimentary, post-depositional, and ore-forming processes. This diversity of occurrences indicates a complex post-depositional evolution and provides important information about the genesis and evolution of the mineralization system.

Diagenetic dolomitization formed texture-destructive ferroan-dolomite as pods and anastomosed veins replacing depositional calcite (Fig. 5a). These anastomosed non-planar textures of iron-bearing dolomite suggest formation during conditions that involved fluids enriched in iron. Syn-ore dolomitization is represented by euhedral to subhedral dolomite crystals within/bordering dissolution seams and those associated with sulfides (Figs. 5b, 6a, 7b). However, copper sulfides are also frequently associated with calcite-bearing host rocks lacking significant amounts of dolomite (Figs. 5b and 8d). Late-ore and post-ore dolomite are hosted in veins that cut syn-ore stage minerals and are, thus, related to later mineralizing fluids. Those associated with the post-ore stage, however, formed barren veins and suggest an inability for further remobilizing sulfides, apart from cinnabar.

Records of multiple dolomitization events in Gortdrum are coherent with regional observations of pervasive dolomitization of the Irish Midlands (Gregg et al., 2001; Hitzman et al., 2002; Johnson et al., 2009; Wilkinson, 2014). Dolomitization intensity has been argued as an important ore formation control separating small size deposits such as the undolomitized Tynagh and Ballinalack from large size and strongly dolomitized deposits such as Lisheen (Hitzman et al., 2002). However, most dolomite in the Irish Midlands is diagenetic, formed during northward-directed fluid propagation at 0.5 to 2.5 km of depth (Hitzman et al., 1998). Therefore, the intensity of dolomitization can be interpreted as a proxy for enhanced porosity and permeability of pre-ore calcareous rocks rather than a proxy for mineralization intensity.

The Navan Deposit is an example of a large mineral deposit in the Irish Midlands where dolomitization and mineralization intensity are uncorrelated (Ashton et al., 2015). In Navan, various ore lenses are hosted in association with undolomitized rocks whereas dolomitic rocks acted as local impermeable barriers to fluid flow instead of as a fluid flow conduit (Braithwaite and Rizzi, 1997; Anderson et al., 1998; Ashton et al., 2015). In Gortdrum, the absent correlation between dolomite and ore sulfide is reflected in the MgO and Cu values (Fig. 10 and Table 1). Syn-ore dolomite is subordinate to the more pervasive diagenetic dolomite and they cannot be differentiated through visual estimation and whole-rock assays. Therefore, we argue that dolomite abundance is a poor proxy for mineralization intensity in the Gortdrum deposit because sulfides are dominantly hosted in calcite-rich rocks and because dolomite formed during various stages in the evolution of the deposit.

8.2. Dissolution and replacement

Dissolution seams and stylolites are ubiquitous in the Gortdrum carbonate-bearing rocks. They can be filled with a combination of sericite, organic matter, chalcedony, and dolomite as confirmed by petrography and EDS analyses. Their cross-cutting relationship with earlier vein stages (Fig. 5a and b) might indicate that they formed after diagenesis of the host rocks. Dissolution seams may host ore sulfides (Figs. 7a, b, 8b) or be spatially associated with them (Figs. 5a, b, 6b), indicating an important role for secondary porosity processes. However, the relationship of sulfides to other dissolution-seam hosted minerals is not straightforward. Sericite, for example, occurs in variable concentrations throughout dissolution seams up to 2 cm thick, and can be easily confused with remobilized argillite layers (Fig. 5a) or as patchy disseminations in sulfide-rich seams (Fig. 7b). Additionally, portions of a single dissolution seam might host both sericite and sulfides, and parts of it host neither (Fig. 7a). Therefore, variations of modal concentrations of sericite along seams are neither indicative of the presence of
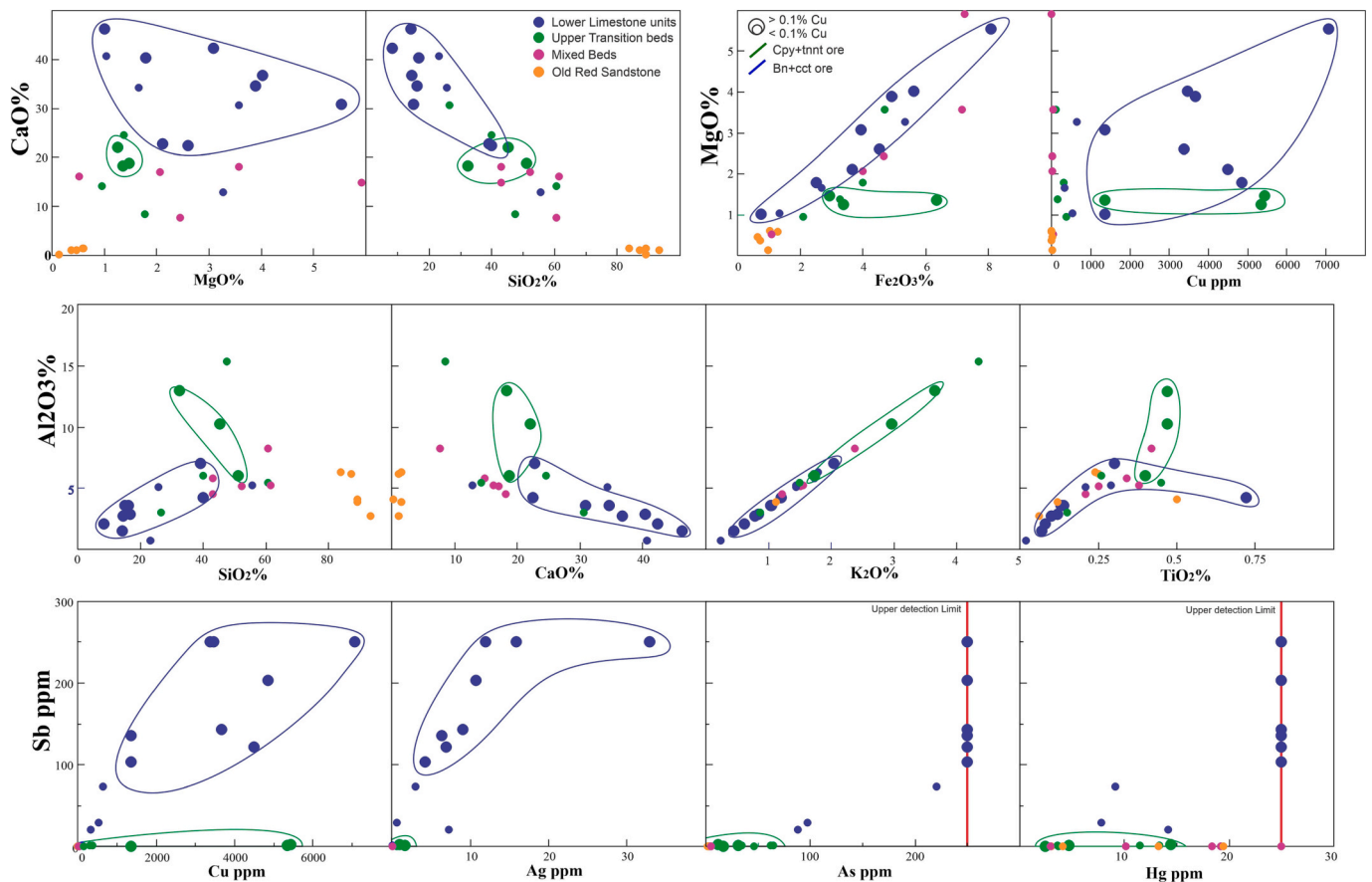
Fig. 10. Binary diagrams of major and relevant chalcophile elements for four groups of Gortdrum Deposit rocks (28 samples) highlighting chemical differences between ore types and between various host rocks. Copper grades representative of the mineralization process (>0.1 % Cu) are shown as larger circles contrasting with small circles for barren rocks and those with <0.1 % Cu grades. Note that the diagrams of major elements show a correlation between those elements and the mineralogical composition of each host rock. For example, the siliciclastic Old Red Sandstone formation contains high SiO_2 and the Lower Limestone Shale high CaO. The MgO content does not show a clear correlation with Cu content. Furthermore, the calcophile elements (Sb, Cu, Ag, As and Hg) show the highest content in the Lower Limestone Shale (Upper ore).

mineralization nor its intensity.

We interpret dissolution-seam as hosted sericite is authigenic and deposited from fluids containing dissolved Si, Al, and K as revealed by the strong positive correlation between the oxides of these elements (Fig. 10), and perhaps also Ti, albeit for the latter results above 0.25 % TiO_2 are skewed due to trace detrital titanite and rutile. Correlation of Si, Al, and K is also strongly positive with trace elements such as Rb, Cs, Nb, Ta, Ga, and Th and, albeit with some data spread, with Ba, V, Cr, Zr, and Hf (Table 1). A similar geochemical footprint was also observed in the hydrothermal feeder zones of Lisheen (Wilkinson et al., 2011). A fluid capable of forming sericite with this chemical association is compatible with prior leaching of both felsic and mafic crustal components.

The relationship of mineralization in the Irish Midlands to the deposition of potassic silicates is still open to interpretation and was detailed by Riegler and McClenaghan (2017). These authors were able to determine a *syn*-ore mineral assemblage including multiple potassic silicates such as phengite, illite, (Ba-K) feldspar, adularia, and albite associated with sphalerite in breccia matrices from Lisheen and Navan ores. Considering the complex potassic silicate assemblage detailed in Navan and Lisheen, our description of sericite in Gortdrum dissolution seams is probably an oversimplification to be resolved by methods outside the scope of the present work. Intense deposition of authigenic potassic silicates might be able to explain certain features of Navan ores, where discrete argillite beds within the Micrite Unit have an unclear origin, whether as an exotic input during the mineralization,

assimilation into the ore of argillite layers (Anderson et al., 1998) or as detrital grains (Peace et al., 2003). Alternatively, they could be the product of authigenic formation and concentration of potassic silicates during mineralization-related dissolution. However, Riegler and McClenaghan (2017) were unable to investigate potassic silicate authigenic deposition in barren rocks. At Gortdrum (this work) and at Navan (Peace et al., 2003), barren rocks surrounding ore zones also contain dissolution seams with potassic silicates. This suggests that the relationship between authigenic silicates and mineralization is not clear.

We interpret that most dissolution seams in Gortdrum, and their mineral filling, are related to the final stages of diagenesis or to a post-diagenetic stage that predated ore deposition. These burial compaction features can be parallel and oblique to the bedding and are subordinate channels for the mineralized fluid in relation to the main vertical flow through the fault damage zones. Sulfide deposition induced fluid acidification and consequent permeability enhancement leading to additional precipitation of sericite in the matrix (Fig. 5b). A similar relationship between sulfide mineralization and the evolution of dissolution seams was described by Peace et al. (2003) for the U lenses of Navan.

8.3. Magmatic influence on mineralization

Mineralization in the province is roughly contemporaneous to magmatic and volcanic activity associated with the Knockroe Formation, which is widespread within the Limerick Basin and surrounding
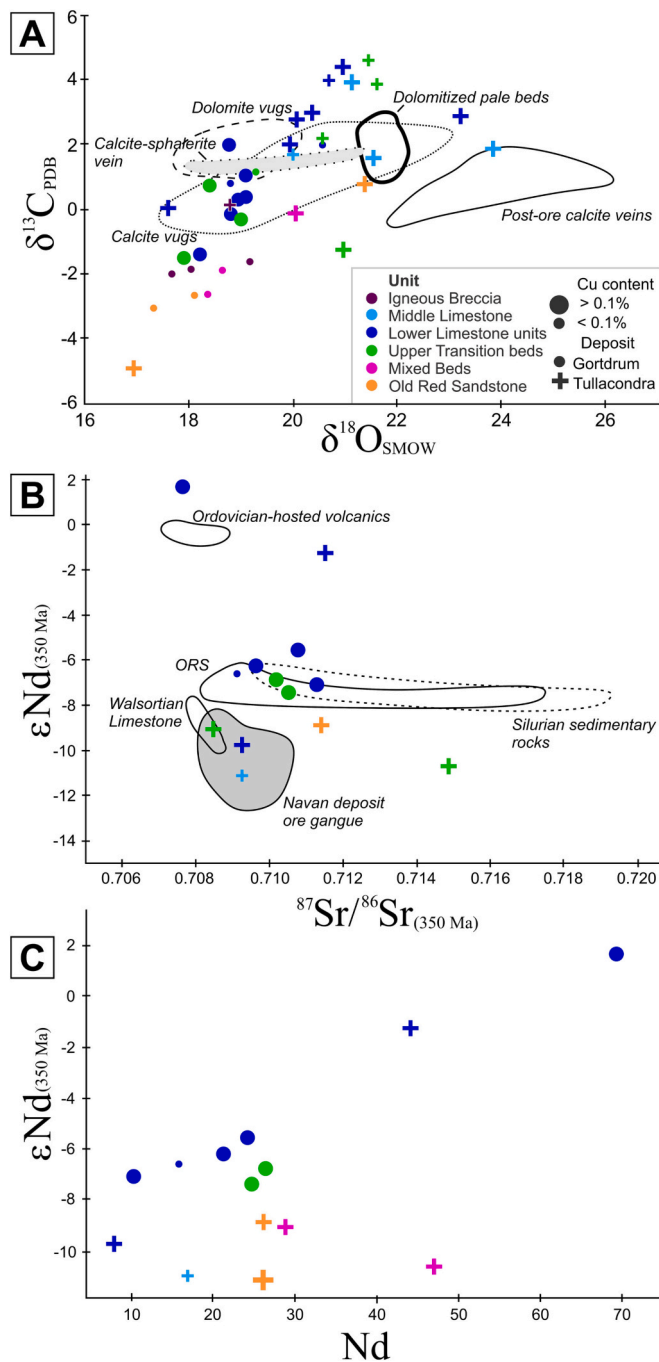
Fig. 11. a) C$_{PDB}$ vs. O$_{SMOW}$ isotopes plot showing samples from the Gortdrum and Tullacondra Cu-Ag deposits and compositional fields from carbonates of the Zn-Pb Navan deposit (Ashton et al., 2015). Note that the results from Tullacondra are higher than from those at Gortdrum. In both cases, carbonate-dominated upper units have higher C and O isotope values compared to the other units. Carbonate-dominant samples from Tullacondra and Gortdrum show similar C-O isotopic ranges with Navan stage 2 calcite vugs associated with the main mineralization stage of Navan; b) εNd (350 Ma) vs. ^{87}Sr/^{86}Sr (350 Ma) plot for Gortdrum and Tullacondra samples compared to outlines from Navan and regional results (Walshaw et al., 2006). Gortdrum and Tullacondra have similar restricted ranges of initial εNd, but Tullacondra shows more variable initial ^{7}Sr/^{86}Sr. The anomalies are observed in the Ballyvergin Shale in Gortdrum and close to the Ballyvergin Shale in Tullacontra. Gortdrum Sr-Nd compositions resemble those from barren Old Red Sandstone and Silurian metasedimentary rocks from Navan. On the other hand, the ^{143}Nd/^{144}Nd ratios from Tullacondra are compatible with data from Navan gangue and ^{87}Sr/^{86}Sr with the Old Red Sandstone samples from Navan; c) εNd (350 Ma) vs. Nd plot

indicating high values in both axes for samples from the base of the Lower Limestone Unit.

regions (Somerville et al., 1992; Elliott et al., 2015; Wilkinson and Hitzman, 2015). The Gortdrum Deposit, for example, contains altered dikes and igneous breccias detailed by Steed (1975) that could represent subvolcanic equivalents of the Knockroe Formation. Therefore, a discussion of igneous rocks and their associated products in Gortdrum can provide clues to the elusive relationship between magmatism and mineralization in the deposit.

Igneous activity is represented in Gortdrum by the 'Main Dike', which is, in fact, a 5 to 9 m thick zone of multiple dikes of altered mafic rocks, all striking approximately *E*-W (Fig. 1c). Carbonate rocks hosting these dikes can be strongly dolomitized and contain high-grade mineralization, as indicated by legacy geochemical data (e.g., Steed, 1986). However, the bulk of mineralization is hosted within carbonate breccias along the Gortdrum Fault. Clastic breccias (Fig. 9b), sometimes with mineralized clasts, are common around these dikes. Breccias can also cut dikes and contain angular clasts of mafic rocks. This cross-cutting relationship suggests that brecciation is related to a later event that postdates magmatic emplacement.

Our Sr-Nd isotopes data suggests more than two samples with outlier compositions compatible with a mantle-like derivation that could be, at first glance, evidence for igneous influence. In Gortdrum, this corresponds to a mineralized sample from the Ballyvergin Shale (Fig. 11b) at the top of the Lower Limestone Unit with positive εNd. Otherwise, most Gortdrum samples show Sr-Nd compositions compatible with the Old Red Sandstone from Walshaw et al. (2006). Tullacondra also has an outlier with higher εNd than other samples, which was equally collected from the top of the Lower Limestone Unit. Further investigation of the Gortdrum anomalous samples indicates a positive relationship between εNd and Nd (Fig. 11c), and Nb, Ta, Y, Zr, and Th, which are immobile elements unlikely to be easily transported by hydrothermal fluids. We interpret that these mantle-like compositions are associated with detrital zircon, rutile, or other accessory minerals eroded from different source areas and, thus, unrelated to mineralization.

Therefore, evidence for a genetic relationship in Gortdrum between magmatism and mineralization - beyond spatial proximity - is lacking. If Gortdrum mineralization processes were related to magmatic fluids, a shift towards lower oxygen isotope values would be expected, as observed in skarns where δ^{18}O$_{SMOW}$ shifts from compositions compatible with marine carbonates (>20 ‰) to lower values under re-equilibration with magmatic fluids (Du et al., 2017). The oxygen isotope range for Gortdrum (and Tullacondra) is compatible with Navan data, where mineralization is associated with the mixing of basinal and meteoric fluids (Ashton et al., 2015; Yesares et al., 2019). Gortdrum carbon and oxygen isotope data show that dike emplacement was unable to modify carbonate isotopic compositions. Any potential hydrothermal influence from this magmatism was unrelated to mineralization and had an exceptionally low fluid/rock ratio. We favor an interpretation that mineralizing fluids variably modified the C-O composition of host rocks but that their original composition was generally compatible with ranges observed in the basin. The Sr-Nd system was unaffected by these fluids, or more dramatic detrital-related controls masked them.

Mafic dikes were likely overprinted by mineralization instead of representing their source, rendering magmatism an unlike source for copper and sulfur. However, regional magmatism could have acted as a heat source, allowing enhanced circulation of metal-bearing fluids, as Wilkinson and Hitzman (2015) suggested for the Irish Midlands.

8.4. Ore formation controls

The plumbing system created by the Gortdrum Fault and related damage zone permeability is the most noteworthy ore formation control, which allowed fluids from the Munster Basin siliciclastic rocks and the
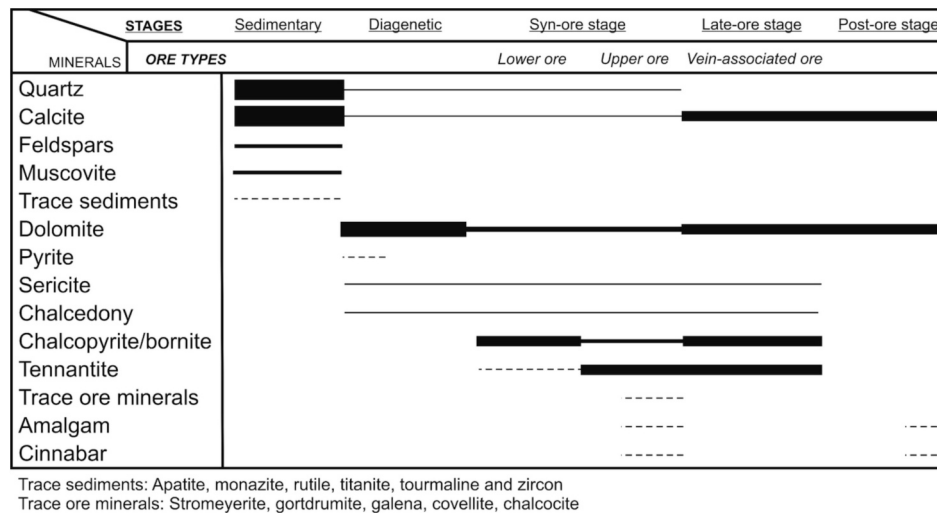
STAGES	Sedimentary	Diagenetic	Syn-ore stage		Late-ore stage	Post-ore stage
MINERALS / ORE TYPES			Lower ore	Upper ore	Vein-associated ore	
Quartz						
Calcite						
Feldspars						
Muscovite						
Trace sediments						
Dolomite						
Pyrite						
Sericite						
Chalcedony						
Chalcopyrite/bornite						
Tennantite						
Trace ore minerals						
Amalgam						
Cinnabar						

Trace sediments: Apatite, monazite, rutile, titanite, tourmaline and zircon
Trace ore minerals: Stromeyerite, gortdrumite, galena, covellite, chalcocite

Fig. 12. Paragenetic sequence of the Gortdrum Cu-Ag deposit.

Silurian basement to seep into carbonate-bearing rocks of the Lower Limestone Shale Formation. After encountering carbonate-dominant rocks for the first time upon ascension, mixed-fluid reaction with carbonates rendered dissolved metals unstable in solution and they precipitated as sulfides. For fluid mixing, as in other systems, an adequate permeable structure is essential to carry the flow of two fluids (brines and meteoric water/groundwater) in the same volume of rock and allow efficient mixing to occur. For systems hosted in faulted sedimentary rocks, according to Wilkinson and Hitzman (2015), this requires a non-sealing fault type with a wide damage zone favored by reactivation periods to rehabilitate permeability in contact with carbonates. The capacity of fluids to dissolve carbonates decreased away from feeders but was enhanced by secondary faults and fractures of the damage zone, and fluid flow along bedding and reactivated dissolution seams.

Hydrothermal fluids ascend through these normal faults as warm, H_2S-poor fluids scavenging metals from the Lower Paleozoic basement rocks (Wilkinson et al., 2015; Ashton et al., 2015; Yesares et al., 2022), subsequently mixing with cooler, hypersaline brine with dissolved sulphate, further reduced by bacteria at or near the site of sulfide precipitation (Anderson et al., 1998; Blakeman et al., 2002; Ashton et al., 2015). This fluid mixing model suggests that the rising hydrothermal fluids also react with brines present in the host rock strata creating a horizontal zone of increased carbonate dissolution and precipitating out metals.

Two main cross-cutting plumbing stages took place during the development of the Gortdrum Fault: a) the earlier *syn*-ore stage associated with bedding- and dissolution-seams parallel flow and; b) the later system associated with fracturing and vein deposition. The fault movements and development likely separated these two stages, which allowed carbonate cementing of the early plumbing system, as expected during the inter-seismic phase (Woodcock et al., 2007). Later fault development and associated fracturing created renewed permeability and allowed mineralizing fluids to flow along and precipitate the vein-associated ore. We interpret that ore deposition in Gortdrum occurred in episodes or stages during the Irish Midlands Basin extension, rather than as continuous sulfide deposition, which might favor a larger sulfide concentration.

Therefore, ore deposition in Gortdrum can be associated with four stages in the evolution of the host rocks and the mineralizing system:

a) **Sedimentary/Diagenetic stage**: the deposition of dominantly carbonate-rocks of the Lower Limestone Shale Formation on top of siliciclastic sedimentary rocks of the Munster Basin created a sharp chemical contrast but also an important difference in structural competency. Burial and diagenesis generated localized dolomitization, veining and development of dissolution seams.

b) **Syn-ore stage**: The syn-ore stage included percolation of a first fluid pulse that were capable of depositing chalcopyrite, bornite and chalcocite (as the lower ore) upon meeting the lowermost carbonate-bearing unit (the Transition Series). Probably, a second fluid pulse contained a much more diverse metal content including As, Ag, Sb and Hg, in addition to Cu, which deposited as tennantite rimming trace of bornite and chalcopyrite (Fig. 6d and e) as the upper ore, dominantly within Lower Limestone units. The syn-ore stage ended with the cessation of extensional faulting and consequent sealing of the mineralizing plumbing system.

c) **Late-ore stage**: The late-ore stage commenced with reactivation of the fault after episodic sealing of permeability. This reactivation induced additional fracturing of the sequence with the more competent limestones of the Lower Limestone units fracturing more efficiently than the Transition Series clay-rich rocks. Fault-induced fracturing created enough permeability, becoming a conduit and occurring the deposition of the vein-associated ore containing similar mineralogy to that of the upper ore but with crosscutting relationships.

d) **Post-ore stage**: Post-ore stage barren, calcite-dominant veining (types 2 and 3) developed during non-mineralized fluid flow associated with later tectonic activity, such as Variscan deformation.

9. Comparison with other deposits

The Gortdrum deposit shares important features with other Cu-Ag occurrences in the Irish Midlands such as Tullacondra (Wilbur and Carter, 1986; Silva et al., 2021), Aherlow (Romer, 1986), and Ballyvergin (Andrew, 1986; Colthrust and Reed, 2019) where: a) copper sulfides with variable pyrite and trace of galena and sphalerite are hosted at the base of the Lower Limestone Shale Formation, and b) the ore envelope is either limited by fault zones, or it is strongly controlled by them (Aherlow). Spatial association with magmatic rocks is not a determining factor in this group of deposits as igneous rocks are common in Gortdrum and limited in Tullacondra but have not been described in Aherlow and Ballyvergin. These mineral occurrences suggest that Cu-Ag mineralizing fluids existed in the Irish Midlands, where they could be channeled through faults and fracture zones and deposit as sulfides when they came into contact with reactive carbonate-bearing rocks. Probably, copper-rich fluid circulated in the Munster Basin even before the deposition of Paleozoic carbonate sequences, as attested by

vein-hosted copper deposits in Allihies formed around 366 Ma (Lang et al., 2020) and our work shows that it was still circulating after the deposition of the Lower Limestone Shale Formation.

Some of the described Gortdrum mineralization characteristics, such as mineralogy and geochemical footprint, are common in stratiform copper deposits in central Africa and Poland (Hitzman et al., 2005). In these deposits, saline Cu-bearing basinal fluids flowing through redbeds can reduce during reaction with carbonate rocks or organic matter in upper strata and precipitate sulfides to form small to world-class copper deposits. Upward escape of metal-bearing fluids is limited by capping sediments with low permeability, allowing these fluids to convect through the basin continuously. Large stratiform copper deposits probably formed under hydrological closed systems that fostered longer convection periods and reacted with ample areas of reductant-rich strata (Hitzman et al., 2005). In the growth-fault abundant basin envisioned for the Irish Midlands, perhaps the capping role of sediments such as the Ballyvergin Shale would be limited by fault-enhanced permeability. This hydrological connectivity would hinder the continuous convection of metal-bearing fluids and create, instead, episodic mineralization. If this mineralization model can be applied for the Irish Midlands, the challenge is to locate areas where faulting was limited during fluid-flow. However, growth fault inversion during Variscan compression creates additional breaches of the hydrological system, likely limiting the duration of a closed hydrological system.

Irish-type mineralization is an obvious choice of style to compare with Gortdrum and similarities go beyond the common deposition at the base of the Irish Midlands basin. Examples such as Navan, Lisheen, Silvermines, and Tynagh are Zn-Pb deposits, but they contain minor copper and silver late-ore stage mineralization associated with feeder zones. At Silvermines and Lisheen, high Cu-Ag areas are associated with structurally complex fault lenses with high permeability due to fracture density (Kyne et al., 2019). These areas are interpreted as small-scale breaching of early-stage relay ramps that acted as feeder zones for mineralizing fluids. At Lisheen, the four feeder zone areas show anomalous Cu and Ag, and also As, Ni, Co, and Cd, and were likely a single feeder point along the normal fault before reverse activation (Torremans et al., 2018). Elevated concentrations of these elements away from feeder zones are lacking in the rest of Lisheen (Torremans et al., 2018). In both Lisheen and Silvermines deposits, the geometry and degree of breaching play a crucial role in creating an appropriate piping system for upwelling mineralized fluids (Kyne et al., 2019). At Tynagh, tennantite, galena, and barite with subordinate chalcopyrite, bornite, and arsenopyrite were deposited as irregular shaped massive bodies. This mineral assemblage is associated with a separate and later mineralization stage deposited at Zone 2, at the immediate hanging wall of the Main Fault, where grades reached up to 0.5 % Cu (Boast et al., 1981; Clifford et al., 1986). In similarity with Gortdrum, this high-Cu zone is also characterized by elevated Hg and Ag associated with copper minerals.

Abundant Zn and Pb are the most conspicuous missing Irish-type ingredients in the Gortdrum deposit and other similar occurrences. Our petrography and whole-rock geochemical data for Gortdrum show a weak positive correlation between Cu and Zn (up to 800 ppm) and Pb (40 ppm) (Table 1), and similar results and ranges are observed in Tullacondra (Silva et al., 2021). In a study of geochemical haloes around the Gortdrum deposit using exploration data, Steed and Tyler (1979) indicated a clear predominance of Cu-Ag-Hg around Gortdrum but a Waulsortian-hosted Zn and Pb dispersion halo 1 km to the NE along the Gortdrum Fault. A similar dispersion pattern is observed in areas around Tullacondra, where shallow soil geochemical Zn-Pb anomalies above 100 ppm occur along-trend. Also, Zn-Pb occurrences can be found at the Grange East target, 4 Km east of Tullacondra, where small pockets of mineralization grade up to 6.8 % Zn and 1.7 % Pb within sub-Waulsortian limestones (Slowey, 2010). Perhaps the clearest example of spatial proximity of Cu-Ag mineralization and Waulsortian-hosted Irish-type Zn-Pb comes from the Ballyvergin deposit, 5 km to the NE of Kilbricken with an indicated resource of 2.65 Mt @ 4.7 % Zn, 2.9 %

Pb, 50 g/t Ag, 0.3 % Cu calculated with a 5 % Zn equivalent cut-off (Colthrust and Reed, 2019). Another 5 km ESE of Ballyvergin lies the Milltown occurrence where a drill hole intersected 13.3 m @ 10.5 % Zn and 5.8 % Pb in the Waulsortian limestones.

The resemblance of textural, geochemical, and isotopic characteristics of Gortdrum and Zn-Pb deposits in the province suggests a similar mineralizing system. Each stage transition can represent variations in structural controls and the nature of mineralizing fluids in a deposit style such as the Irish-type, which is separated into stages with its own mineral assemblage. We argue that Gortdrum, and other similar Cu-Ag deposits, could represent a sub-variety of Irish-type mineralization where only feeder-proximal mineralization formed or was preserved. We argue that, in Gortdrum, the earlier Zn-Pb stage was either absent or seeped out to form outer Zn-Pb disseminations instead of high-sulfide concentrations. Alternatively, a hypothetical earlier Zn-Pb mineralization was never discovered or was eroded off. Other similar examples, such as Ballyvergin, are more clearly spatially related to important Zn-Pb concentrations.

The potential for large Cu-Ag deposits in the Irish Midlands is hard to assess and easy to dismiss when all known occurrences are small and low grade. However, Zn-Pb deposits in the Irish Midlands also vary in size, and the occurrence of only two large deposits (Lisheen and Navan) justifies renewed exploration interest in the province. Perhaps the potential for copper mineralization remains underexplored and should be revisited. Additionally, we argue that the abundance of reductant-rich beds in both Paleozoic carbonate sequences and older siliciclastic could be alternative potential traps for these circulating copper-rich fluids.

10. Conclusions

The Gortdrum epigenetic Cu-Ag(±Sb-Hg) deposit was formed during extension when hot, metal-bearing, hydrothermal fluids flowed upwards using the Gortdrum normal fault as a conduit and precipitated mineralization upon reaction with carbonate-rich rocks of the Lower Limestone Shales. The occurrence of multiple normal faults and emplacement of dikes, diatremes, and igneous breccias in the region suggest local extension during deposition, in agreement with regional interpretations. Local igneous activity in Gortdrum was unable to modify the carbon and oxygen isotope signature of carbonate-hosted ore or barren rocks, suggesting a low fluid/rock ratio of any igneous-related hydrothermal activity. Therefore, magmatism is an unlike source for copper or sulfur, and, instead, fractured dikes/igneous breccias could have acted as alternative fluid conduits and sulfide depositional sites.

We propose a mineralization model where fault development during the *syn*-ore stage created an appropriate plumbing system to channel basinal mineralizing fluids into reductant carbonate-rich rocks. Upon reduction, these fluids precipitated chalcopyrite and bornite within the Transition Series units and formed the lower ore type. A pulse of Cu-Ag fluids also enriched in Ag, Hg, Sb, and As deposited tennantite and secondary sulfosalts in the upper strata (the Lower Limestone units) and formed the upper ore type. The exotic mineral assemblage containing cinnabar, mercury amalgam, gortdrumite, stromeyerite, for which Gortdrum is known in Irish geology, is associated with this type of ore and later remobilization.

Our detailed textural study suggests that fault sealing, by carbonate cement, decreased local permeability and strongly limited the volume of mineralizing fluids available for the development of the lower and upper ores. Renewed fracturing and veining occurred during the late-ore stage, probably associated with an episodic reactivation of the Gortdrum Fault. This late fracturing created secondary permeability which allowed the mineralizing fluids to flow into the favorable host unit and allowed sulfide fracture-filling and deposition of vein-associated ore containing the same mineralogy as the upper ore.

The mineralogy, ore shoot geometry, and geochemical association of Gortdrum are fairly similar to other Cu-Ag deposits in Ireland, such as

Tullacondra, Ballyvergin, and Aherlow. Some of these common traits are also shared with classic Zn-Pb Irish-type deposits such as Navan, Lisheen, Silvermines, and Tynagh, where copper-silver ores are proximal to feeder faults from the larger zinc-lead mineralization. In these Irish-type deposits, copper-silver mineralization is associated with variable amounts of late-stage chalcopyrite and tennantite, deposited after the main Zn-Pb mineralization stage. Additionally, copper ores in these large Zn-Pb systems are systematically enriched in Ag and As, and sometimes in Sb and Hg, similar to the Gortdrum geochemical footprint.

We argue that these chemical and mineralogical similarities, in conjunction with our C-O and Sr-Nd results, suggest that Gortdrum could represent a variation of the Irish-type system where Cu-Ag-Sb-bearing fluids succeeded in forming a deposit. Hypothetical early-stage Zn-Pb fluids a) never existed; b) deposited disseminated sulfides in country-rocks, c) formed an undiscovered resource, or, d) deposited ore concentrations later eroded off. Considering the various locations containing Cu-Ag mineralization in Ireland, these metals were abundant in the fluids percolating through the basin. Therefore, the potential for large copper-silver deposits in the province can be investigated in carbonate-bearing Paleozoic rocks of the Irish Midlands using the similarities with Zn-Pb Irish-type deposits as a starting point. Additionally, older siliciclastic strata containing organic matter, such as Devonian and Silurian sedimentary rocks underneath the Irish Midlands, may also be potential underexplored targets.

Supplementary data to this article can be found online at https://doi.org/10.1016/j.gexplo.2023.107196.

Funding

CRediT authorship contribution statement

Conception and design of the study: P. Cordeiro, A. M. Santos, P. Meere, R. Unitt

Acquisition of data: P. Cordeiro, A. M. Santos, L. Corcoran, A. Simonetti

Analysis and interpretation of data: G. Steed, A. M. Santos, A. A. Silva

Drafting of the manuscript: P. Cordeiro, A. M. Santos, A. A. Silva

Revising the manuscript: A. M. Santos, A. A. Silva

Approval of the version of the manuscript to be published: P. Cordeiro, A. M. Santos, G. Steed, A. A. Silva, P. Meere, L. Corcoran, A. Simonetti, R. Unitt

Declaration of competing interest

The authors declare that they have no known competing financial interests or personal relationships that could have appeared to influence the work reported in this paper.

Data availability

Data will be made available on request.

Acknowledgements

References

ALS Global, 2016. Geochemistry schedule of services and fees, 52 pp. https://cdn-als.dataweavers.io/-/media/als/resources/services-and-products/geochemistry/fee-schedules/als-geochemistry-fee-schedule-usd.pdf?rev=24db94b2a185421693cd95fd27a4f4b2.

Anderson, I.K., Ashton, J.H., Boyce, A.J., et al., 1998. Ore depositional processes in the Navan Zn-Pb deposit, Ireland. Econ. Geol. 93, 535–563. https://doi.org/10.2113/gsecongeo.93.5.535.

Andrew, C.J., 1986. The geological setting and style of mineralization at Ballyvergin, County Clare. In: Andrew, C.J., Crowe, R.W.A., Finlay, S. (Eds.), Geology and Genesis of Mineral Deposits in Ireland. Irish Association for Economic Geology, Dublin, pp. 475–480.

Ashton, J.H., Blakeman, R.J., Geraghty, J.F., 2015. The giant Navan carbonate-hosted Zn-Pb deposit - a review. In: Archibald, S.M., Piercey, S.J. (Eds.), Current Perspectives on Zinc Deposits. Geological Survey of Ireland, Dublin, pp. 17–35.

Ashton, J.H., Downing, D.T., Finlay, S., 1986. The geology of the Navan Zn-Pb orebody. In: Andrew, C.J., Crowe, R.W.A., Finlay, S. (Eds.), Geology and Genesis of Mineral Deposits in Ireland. Irish Association for Economic Geology, Dublin, pp. 243–280.

Balboni, E., Jones, N., Spano, T., Simonetti, A., Burns, P.T., 2016. Chemical and Sr isotopic characterization of North America uranium ores: Nuclear forensic applications. Appl. Geochem. 74, 24–32.

Blakeman, R.J., Ashton, J.H., Boyce, A.J., Fallick, A.E., Russell, M.J., 2002. Timing of interplay between hydrothermal and surface fluids in the Navan Zn+Pb orebody, Ireland: evidence from metal distribution trends, mineral textures and δ34S analyses. Econ. Geol. 97, 73–91. https://doi.org/10.2113/gsecongeo.97.1.73.

Boast, A.M., Coleman, M.L., Halls, C., 1981. Textural and stable isotopic evidence for the genesis of the Tynagh base metal deposit, Ireland. Econ. Geol. 76 (1), 27–55.

Braithwaite, C.J.R., Rizzi, G., 1997. The geometry and petrogenesis of hydrothermal dolomites at Navan, Ireland. Sedimentology 44, 421–440. https://doi.org/10.1046/j.1365-3091.1997.d01-30.x.

Çimen, O., Kuebler, C., Simonetti, S.S., Corcoran, L., Mitchell, R., Simonetti, A., 2019. Combined boron, radiogenic (Nd, Pb, Sr), stable (C, O) isotopic and geochemical investigations of carbonatites from the Blue River Region, British Columbia (Canada): Implications for mantle sources and recycling of crustal carbon. Chem. Geol. 529, 119240.

Clifford, J.A., Ryan, P., Kucha, H., 1986. A review of the geological setting of the Tynagh orebody Co. Galway. In: Andrew, C.J., Crowe, R.W.A., Finlay, S. (Eds.), Geology and Genesis of Mineral Deposits in Ireland. Irish Association for Economic Geology, Dublin, pp. 419–439.

Colthrust, J., Reed, G., 2019. Technical Report (Amended and Restated) on the Mineral Resource Estimate for the Kilbricken Zinc-silver-lead-copper Project Co. Claire, Ireland for Hannah Metals, LTD. NI-43-101 Report.

Du, L.J., Li, B., Huang, Z.L., Zhou, J.X., Zou, G.F., Yan, Z.F., 2017. Carbon-oxygen isotopic geochemistry of the Yangla Cu skarn deposit, SW China: implications for the source and evolution of hydrothermal fluids. Ore Geol. Rev. 88, 809–821.

Duane, M.J., 1988. Genesis, mineralogy and geochemistry of uranium in the Gortdrum stratiform copper deposit, Ireland. Mineral. Deposita 23, 50–57. https://doi.org/10.1007/BF00204228.

Elliott, H.A.L., Gernon, T.M., Roberts, S., et al., 2019. Diatremes act as fluid conduits for Zn-Pb mineralization in the SW irish ore field. Econ. Geol. 114, 117–125. https://doi.org/10.5382/econgeo.2019.4622.

Elliott, H.A.L., Gernon, T.M., Roberts, S., Hewson, C., 2015. Basaltic maar-diatreme volcanism in the lower Carboniferous of the Limerick Basin (SW Ireland). Bull. Volcanol. 77 https://doi.org/10.1007/s00445-015-0922-2.

Fusciardi, L.P., Guven, J.F., Stewart, D.R.A., Carboni, V., Walsh, J.J., 2004. The geology and genesis of the Lisheen Zn-Pb deposit, Co. Tipperary, Ireland. In: Kelly, J.G., Andrew, C.J., Ashton, J.H., Boland, M.B., Fusciardi, L.P., Stanley, G. (Eds.), Europe's Major Base Metal Deposits. Irish Association for Economic Geology Special Publications, Dublin, pp. 255–282.

Unpublished geological map and technical report of 1971 made available by the company, 1971. Gortdrum Mines Ltd.

Gregg, J.M., Shelton, K.L., Johnson, A.W., et al., 2001. Dolomitization of the Waulsortian Limestone (Lower Carboniferous) in the Irish Midlands. Sedimentology 48, 745–766. https://doi.org/10.1046/j.1365-3091.2001.00397.x.

Hitzman, M.W., Allan, J.R., Beaty, D.W., 1998. Regional dolomitization of the Waulsortian limestone in southeastern Ireland: evidence of large-scale fluid flow driven by the Hercynian orogeny. Geology 26, 547. https://doi.org/10.1130/0091-7613(1998)026<0547:RDOTWL>2.3.CO;2.

Hitzman, M., Kirkham, R., Broughton, D., Thorson, J., Selley, D., 2005. The Sediment-Hosted Stratiform Copper Ore System. https://doi.org/10.5382/AV100.19.

Hitzman, M.W., Redmond, P.B., Beaty, D.W., 2002. The carbonate-hosted Lisheen Zn-Pb-Ag deposit, County Tipperary, Ireland. Econ. Geol. 97, 1627–1655. https://doi.org/10.2113/gsecongeo.97.8.1627.

Hnatyshin, D., Creaser, R.A., Wilkinson, J.J., Gleeson, S.A., 2015. Re-Os dating of pyrite confirms an early diagenetic onset and extended duration of mineralization in the Irish Zn-Pb ore field. Geology 43, 143–146. https://doi.org/10.1130/G36296.1.

Johnson, A.W., Shelton, K.L., Gregg, J.M., et al., 2009. Regional studies of dolomites and their included fluids: recognizing multiple chemically distinct fluids during the complex diagenetic history of lower Carboniferous (Mississippian) rocks of the Irish

Zn-Pb ore field. Mineral. Petrol. 96, 1–18. https://doi.org/10.1007/s00710-008-0038-x.

Johnston, J.D., 1999. Regional fluid flow and the genesis of Irish Carboniferous base metal deposits. Mineral. Deposita 34, 571–598. https://doi.org/10.1007/s001260050221.

Maghfouri, S., Hosseinzadeh, M.R., Choulet, F., 2020. Supergene nonsulfide Zn–Pb mineralization in the Mehdiabad world-class sub-seafloor replacement SEDEX-type deposit, Iran. Int. J. Earth Sci. 109, 2531–2555. https://doi.org/10.1007/s00531-020-01916-7.

Maghfouri, S., Hosseinzadeh, M.R., 2018. The early cretaceous Mansourabad shale-carbonate hosted Zn–Pb (-Ag) deposit, Central Iran: an example of vent-proximal sub-seafloor replacement SEDEX mineralization. Ore Geol. Rev. 95, 20–39. https://doi.org/10.1016/j.oregeorev.2018.02.020.

Maghfouri, S., Hosseinzadeh, M.R., Choulet, F., Alfonso, P., Zadeh, A.M.A., Rajabi, A., 2019. Vent-proximal sub-seafloor replacement clastic-carbonate hosted SEDEX-type mineralization in the Mehdiabad world-class Zn-Pb-Ba-(Cu-Ag) deposit, southern Yazd Basin, Iran. Ore Geol. Rev. 113, 103047 https://doi.org/10.1016/j.oregeorev.2019.103047.

Naylor, D., Shannon, P.M., 2011. Petroleum Geology of Ireland. Dunedin, Edinburgh.

Kyne, R., Torremans, K., Güven, J., Doyle, R., Walsh, J., 2019. 3-D modeling of the lisheen and silvermines deposits, County Tipperary, Ireland: insights into structural controls on the formation of Irish Zn-Pb deposits. Econ. Geol. 114 (1), 93–116.

Lang, J., Meere, P.A., Unitt, R.P., Johnson, S.C., Solferino, G., Torremans, K., Kyne, R., 2020. The vein-hosted copper deposits of the Allihies mining area, SW Ireland; a new structural and chronological evaluation. J. Geol. Soc. 177 (4), 671–685.

Peace, W.M., Wallace, M.W., Holdstock, M.P., Ashton, J.H., 2003. Ore textures within the U lens of the Navan Zn-Pb deposit, Ireland. Mineral. Deposita 38, 568–584. https://doi.org/10.1007/s00126-002-0340-1.

Phillips, W.E.A., Sevastopulo, G.D., 1986. The stratigraphic and structural setting of Irish mineral deposits. Geol. Genes. Miner. Depos. Irel. 1–30.

Pickard, N.A.H., Rees, J.G., Strogen, P., et al., 1994. Controls on the evolution and demise of lower Carboniferous carbonate platforms, northern margin of the Dublin Basin, Ireland. Geol. J. 29, 93–117. https://doi.org/10.1002/gj.3350290202.

Riegler, T., McClenaghan, S.H., 2017. Authigenic potassic silicates in the Rathdowney Trend, Southwest Ireland: new perspectives for ore genesis from petrography of gangue phases in Irish-type carbonate-hosted Zn-Pb deposits. Ore Geol. Rev. 88, 140–155. https://doi.org/10.1016/j.oregeorev.2017.04.017.

Romer, D., 1986. A note on the Aherlow Cu-Ag deposit, County Limerick. In: Andrew, C. J., Crowe, R.W.A., Finlay, S. (Eds.), Geology and Genesis of Mineral Deposits in Ireland, Geology and genesis of mineral deposits in Ireland. Irish Association for Economic Geology, Dublin, pp. 509–511.

Sevastopulo, G.D., Wyse Jackson, P.N., 2009. Carboniferous: Mississippian (Tournasisian and Viséan). In: Holland, C.H., Sanders, I.S. (Eds.), The Geology of Ireland. Dunedin Academic Press, Edinburgh, pp. 215–268.

Shearley, E., Redmon, P., King, M., Goodman, R., 1996. Geological controls on mineralization and dolomitization of the Lisheen Zn-Pb-Ag deposit, Co. Tipperary, Ireland. Geol. Soc. Lond. 107, 23–33.

Silva, A.A., Cordeiro, P., Johnson, S.C., Lagoeiro, L.E., Corcoran, L., Simonetti, A., Meere, P.A., Unitt, R., Colaço, L.S., Santos, A.M., 2021. The carbonate-hosted Tullacondra Cu-Ag deposit, Mallow, Ireland. Minerals 2021 (11), 560. https://doi.org/10.3390/min11060560.

Slowey, E., 2010. Technical Report on the Mallow Base Metal Exploration Project, Count Cork, Ireland. Internal Unpublished Report.

Somerville, I.D., Strogen, P., 1992. Ramp sedimentation in the Dinantian limestones of the Shannon Trough, Co. Limerick, Ireland. Sediment. Geol. 79, 59–75. https://doi.org/10.1016/0037-0738(92)90004-B.

Somerville, I.D., Strogen, P., Jones, G.L., 1992. Biostratigraphy of Dinantian limestones and associated volcanic rocks in the Limerick Syncline, Ireland. Geol. J. 27, 201–220. https://doi.org/10.1002/gj.3350270302.

Somerville, I.D., Waters, C.N., Collinson, J.D., 2011. South Central Ireland. In: Waters, C. N., Somerville, I.D., Jones, N.S. (Eds.), A Revised Correlation of the Carboniferous Rocks in the British Isles. Geological Society of London, pp. 144–152.

Steed, G.M., 1983. Gortdrumite, a new sulphide mineral containing copper and mercury, from Ireland. Mineral. Mag. 47, 35–36. https://doi.org/10.1180/minmag.1983.047.342.05.

Steed, G.M., 1986. The Gortdrum Cu-Ag-Hg orebody. In: Andrew, C.J., Crowe, R.W.A., Finlay, S. (Eds.), Geology and Genesis of Mineral Deposits in Ireland. Irish Association for Economic Geology, Dublin, pp. 481–499.

Steed, G.M., 1975. The Geology and Mineralization of the Gortdrum District. University of London. Unpublished PhD Thesis.

Steed, G.M., Tyler, P., 1979. Lithogeochemical haloes in Gortdrum. In: Prospecting in Areas of Glaciated Terrain. Inst. Mining Metallurgy, Dublin, pp. 30–39.

Strogen, P., 1988. The carboniferous lithostratigraphy of Southeast County Limerick, Ireland, and the origin of the shannon trough. Geol. J. 23, 121–137. https://doi.org/10.1002/gj.3350230202.

Thompson, I., 1965. The Discovery of the Gortdrum Deposit, CO. Tipperary, Ireland. Internal Unpublished Report.

Torremans, K., Kyne, R., Doyle, R., et al., 2018. Controls on metal distributions at the Lisheen and Silvermines deposits: insights into fluid flow pathways in Irish-type Zn-Pb deposits. Econ. Geol. 113, 1455–1477. https://doi.org/10.5382/econgeo.2018.4598.

Walshaw, R.D., Menuge, J.F., Tyrrell, S., 2006. Metal sources of the Navan carbonate-hosted base metal deposit, Ireland: Nd and Sr isotope evidence for deep hydrothermal convection. Mineral. Deposita 41, 803–819.

Whitney, D.L., Evans, B.W., 2010. Abbreviations for names of rock-forming minerals. Am. Mineral. 95, 185–187. https://doi.org/10.2138/am.2010.3371.

Wilbur, D.G., Carter, J.S., 1986. Cu-Ag mineralization at Tullacondra, Mallow, Co. Cork. In: Andrew, C.J., Crowe, R.W.A., Finlay, S. (Eds.), Geology and Genesis of Mineral Deposits in Ireland. Irish Association for Economic Geology, Dublin, pp. 501–507.

Wilkinson, J.J., 2014. Sediment-hosted zinc-lead mineralization: processes and perspectives: processes and perspectives. In: Turekian, K.K., Holland, H.H. (Eds.), Treatise on Geochemistry, 2nd edn. Elsevier Ltd, Oxford, pp. 219–249.

Wilkinson, J.J., 2003. On diagenesis, dolomitisation and mineralisation in the Irish Zn-Pb orefield. Mineral. Deposita 38, 968–983. https://doi.org/10.1007/s00126-003-0387-7.

Wilkinson, J.J., Crowther, H.L., Coles, B.J., 2011. Chemical mass transfer during hydrothermal alteration of carbonates: controls of seafloor subsidence, sedimentation and Zn-Pb mineralization in the Irish Carboniferous. Chem. Geol. 289, 55–75. https://doi.org/10.1016/j.chemgeo.2011.07.008.

Wilkinson, J.J., Hitzman, M.W., 2015. Current perspectives on zinc deposits. Irish Assoc. Econ. Geol. 17–35.

Wilkinson, J.J., Hitzman, M.W., Archibald, S.M., Piercey, S.J., 2015. In: The Irish Zn-Pb Orefield: The View from 2014. Current Perspectives on Zinc Deposits. Irish Association for Economic Geology, Dublin, pp. 59–72.

Woodcock, N., Strachan, R., 2012. Geological History of Britain and Ireland. Wiley-Blackwell, Oxford.

Woodcock, N.H., Dickson, J.A.D., Tarasewics, J.P.T., 2007. Transient permeability and reseal hardening in fault zones: evidence from dilation breccia textures. Geol. Soc. Spec. Publ. 270, 43–53. https://doi.org/10.1144/GSL.SP.2007.270.01.03.

Yesares, L., Drummond, D.A., Hollis, S.P., 2019. Coupling Mineralogy, Textures, Stable and Radiogenic Isotopes in Identifying Ore-Forming Processes in Irish-Type Carbonate-Hosted Zn – Pb Deposits. https://doi.org/10.3390/min9060335.

Yesares, L., Menuge, J.F., Blakeman, R.J., Ashton, J.H., Boyce, A.J., Coller, D., Farrelly, I., 2022. Pyritic mineralization halo above the Tara Deep Zn-Pb deposit, Navan, Ireland: evidence for sub-seafloor exhalative hydrothermal processes? Ore Geol. Rev. 140, 104415 https://doi.org/10.1016/j.oregeorev.2021.104415.